DOI: 10.26599/FSHW.2026.9251174

Contents lists available at SciOpen

Food Science and Human Wellness

journal homepage: https://www.sciopen.com/journal/2097-0765

China Food Publishing Co.

Original research Bifidobacterium breve LE4 Reduces Alzheimer's Disease Pathology and Confers Neuroprotection by Attenuating Neuroinflammation, Restoring Metabolism, and Preserving Gut Barrier

Liu Yang[#], Yutian Huang[#], Mengling Chen, Yue Leng, Ji Wang, Dayong Ren*

College of Food Science and Engineering, Jilin Agricultural University, Changchun, Jilin Province, China.

ABSTRACT: Emerging evidence implicates gut microbiota dysbiosis in Alzheimer's disease (AD) pathogenesis, suggesting probiotic interventions as a viable therapeutic strategy. This study systematically screened 18 *Bifidobacterium* strains, among which *Bifidobacterium breve LE4* exhibited both potent antioxidant activity and lipopolysaccharide (LPS)-reducing capacity. Using APP/PS1 transgenic mice as an AD model, we comprehensively assessed the neuroprotective effects of *B. breve* LE4. The probiotic treatment significantly ameliorated cognitive impairments, particularly in spatial learning, and concurrently improving anxiety-like behaviors and locomotor activity. Notably, *B. breve* LE4 administration normalized metabolic disturbances, including body weight fluctuations, dyslipidemia, and glucose intolerance. At the molecular level, *B. breve* LE4 exerted potent anti-inflammatory effects by reducing systemic and hippocampal cytokine levels through modulation of the TLR4-NF-κB/NLRP3 signaling pathway. The probiotic intervention preserved intestinal barrier integrity, promoted beneficial gut microbiota remodeling, and enhanced short-chain fatty acids (SCFAs) production. These changes correlated with improved synaptic plasticity and reduced AD pathological markers, including Aβ deposition and tau hyperphosphorylation. Untargeted metabolomics revealed that *B. breve* LE4 administration significantly corrected AD-associated metabolic dysregulation, particularly affecting amino acid and lipid metabolism pathways. Our findings demonstrate that *B. breve* LE4 exerts multi-targeted protective effects against AD progression, providing compelling preclinical evidence for microbiota-based interventions in neurodegenerative diseases.

Keywords: Alzheimer’s disease; *Bifidobacterium breve*; gut microbiota; short-chain fatty acids; neuroinflammation

1. Introduction

Alzheimer's disease (AD) is a progressive neurodegenerative disorder characterized by cognitive and memory decline [1, 2]. According to the International Organization for Alzheimer's Disease, the global prevalence of dementia reached approximately 55 million cases in 2024 [3]. With projections indicating a rise to 139 million by 2050, particularly in low- and middle-income countries [4]. It is expected that this growth will bring a heavy burden to low- and middle-income countries. This anticipated increase poses a substantial socioeconomic burden on healthcare systems. The complex pathogenesis of AD involves multiple pathological hallmarks, including amyloid-β (Aβ) plaque deposition, neurofibrillary tangles (NFTs)

[#]These two authors contributed to the work equally.
***Corresponding author**
rendayong@jlau.edu.cn

Received 21 November 2025
Received in revised from 30 December 2025
Accepted 29 January 2026

composed of hyperphosphorylated tau protein, neuronal loss, and chronic neuroinflammation [5, 6]. Current pharmacological interventions, while constituting the mainstay of AD treatment, demonstrate limited efficacy and are often associated with adverse effects [7, 8]. Notably, no existing therapy can effectively halt or reverse AD progression [9, 10]. Consequently, non-pharmacological approaches have gained prominence due to their superior safety profile, therapeutic potential, and cost-effectiveness.

The gut microbiota plays a pivotal role in modulating the microbiota-gut-brain axis through endocrine, immune, and neural pathways [11]. Comparative analyses have revealed significant alterations in the gut microbial composition of AD patients, including reduced alpha diversity, decreased Firmicutes and Actinobacteria abundance, elevated Bacteroides levels, and diminished *Bifidobacterium* populations [12, 13]. Such dysbiosis has been linked to both intestinal and systemic disorders, including metabolic and immune-mediated conditions, while also exacerbating cognitive impairment [14, 15]. During AD progression, gut microbial communities undergo dynamic compositional changes. Of particular concern is lipopolysaccharide (LPS), a proinflammatory endotoxin produced by Gram-negative bacteria, which compromises blood-brain barrier (BBB) integrity and promotes neural dysfunction [16]. Gut dysbiosis increases intestinal permeability, facilitating systemic translocation of bacterial products such as LPS. This process triggers immune cell activation and proinflammatory cytokine release, ultimately promoting neuroinflammation, microglial activation, and exacerbation of Aβ and tau pathology. Importantly, gut microbiota-derived metabolites, particularly short-chain fatty acids (SCFAs), can counteract LPS-induced inflammation by modulating the ERK/JNK/NF-κB signaling pathway (Qian et al., 2022), thereby attenuating Aβ aggregation, tau hyperphosphorylation, and neuroinflammation through multiple mechanisms [17, 18], with consequent improvements in cognitive function. These findings highlight the feasibility of intervening in the progression of AD by regulating the gut microbiota.

Probiotic supplementation has emerged as a promising therapeutic approach for AD management [19-21]. Among various probiotics, *Bifidobacterium* species have attracted considerable research interest due to their demonstrated benefits in gut health maintenance [22], immune modulation [23], and metabolic regulation [24]. Notably, *Bifidobacterium* strains exhibit neuroprotective potential through multiple mechanisms, including cognitive enhancement, amyloidosis reduction via immune modulation, metabolic improvement, and neuroinflammation attenuation. Preclinical and clinical studies have confirmed that specific *Bifidobacterium* strains, such as *B. bifidum* BGN4 and B. longum BORI, significantly inhibit amyloidosis and apoptosis while modulating neuroinflammatory responses [25]. These strains also enhance synaptic plasticity, ameliorating cognitive deficits in AD models. *B. breve* A1 administration has been shown to reverse behavioral abnormalities in AD mice [26], suppressing Aβ-induced hippocampal inflammation and improving cognitive performance in human subjects [27, 28]. However, substantial inter-strain variability in therapeutic efficacy necessitates individualized evaluation of each strain's potential.

Despite growing evidence linking gut microbiota alterations to AD pathology, the precise mechanisms underlying microbiota-mediated modulation of brain pathology through intestinal barrier regulation,

immune-inflammatory responses, glial activation, and metabolite signaling remain incompletely understood. We previously isolated eighteen *Bifidobacterium* strains from healthy infant feces and identified a new strain (*Bifidobacterium breve* LE4) as the most promising candidate due to its superior *in vitro* antioxidant capacity and LPS production inhibition. In this study, we further investigated the therapeutic effects and molecular mechanisms of *B. breve* LE4 in APP/PS1 mice. Our investigation focused on *B. breve* LE4-induced modifications in gut microbial composition and their consequences for intestinal barrier integrity, NF-κB pathway activation, NLRP3 inflammasome formation, neuroinflammation, and cognitive function. Additionally, we explored the role of microbiota-derived short-chain fatty acids in neuroinflammatory modulation. This research aims to delineate the unique mechanism by which *B. breve* LE4 targets neuroinflammation through TLR4-NF-κB/NLRP3 inflammasome pathway inhibition, thereby providing a theoretical framework for strain-specific AD interventions.

2. Materials and Methods

2.1 Strain Culture and Preparation of Cell-Free Supernatant, Intact Cells, and Cell-Free Extracts

The eighteen *Bifidobacterium* strains, isolated from the feces of children aged 0 -3 years, were anaerobically cultured in modified De Man, Rogosa, and Sharpe (MRS) medium at 37°C for 48 h. After centrifugation at 4,200 rpm for 20 minutes, the supernatant was filtered through a 0.22 μm membrane to obtain the cell-free supernatant. The bacterial pellet was washed three times with 0.01 M sterile PBS and resuspended to a concentration of 1×10^9 CFU/mL. One aliquot was retained as intact cells, while the other was subjected to ultrasonic disruption (400 W, 5 s on/5 seconds off, 60 cycles) on ice. The resulting supernatant was collected as the cell-free extract following centrifugation at 4,200 rpm for 10 min at 4°C.

2.2 Screening of Antioxidant Activity of Bifidobacteria In Vitro

2.2.1 Determination of DPPH Free Radical Scavenging Ability

In accordance with the methodology established by Despina et al. (2023), 1 mL of cell-free supernatant, intact cells, and cell-free extracts were prepared from *B. breve* LE4 cultures and combined with 1 mL of 0.2 mmol/L DPPH in ethanol. The mixture was incubated in the dark at room temperature for 30 minutes, followed by centrifugation at 10,000 rpm for 1 minute. The absorbance of the supernatant was subsequently measured at 517 nm. The formula utilized for calculations is as follows:

$$\text{DPPH scavenging activity (\%)} = 1-(1-\frac{A1-A2}{A0})\times 100$$

In the formula, A0 represents the absorbance of the control group, A1 represents the absorbance of the sample group, and A2 represents the absorbance of the blank group.

2.2.2 Determination of the Free Radical Scavenging Ability of $ABTS^+$

For the determination of $ABTS^+$ scavenging ability (Seonyoung et al., 2022), $ABTS^+$ was prepared by reacting 7 mmol/L ABTS with 2.45 mmol/L potassium persulfate and incubating the mixture for 16 h in the dark. The resulting $ABTS^+$ solution was then diluted to an absorbance of 0.7 at 734 nm. Subsequently, 2 mL of

the cell-free supernatant, intact cells, and cell-free extracts were pepared form *B. breve* LE4 cultures and added to 4 mL of the $ABTS^+$ solution, followed by incubation for 5 minutes, after which the absorbance was measured at 734 nm. The formula utilized for calculations is as follows:

$$ABTS^+ \text{ scavenging activity } (\%)=1-(1-\frac{A1-A2}{A0})\times 100$$

In the formula, A0 represents the absorbance of the control group, and A1 represents

The absorbance of the sample group, and A2 represents the absorbance of the blank group.

2.2.3 Determination of Hydroxyl Radical Scavenging Ability

The hydroxyl radical scavenging ability of *B. breve* LE4 was assessed by sequentially mixing 1 mL of cell-free supernatant, intact cells, and cell-free extracts with 9 mmol/L salicylic acid, 0.05 mol/L $FeSO_4$, and 8.8 mmol/L H_2O_2. The mixture was incubated at 37°C for 30 min, and the absorbance was measured at 510 nm (Ameer et al., 2018). The formula utilized for calculations is as follows:

$$\bullet OH \text{ scavenging activity}(\%)=\left(1-\frac{A1-A0}{A2-A0}\right)\times 100$$

In the formula, A0 represents the absorbance of the control group, A1 represents the absorbance of the sample group, and A2 represents the absorbance of the blank group.

2.3 Screening of Bifidobacterium Strains with LPS-Inhibitory Activity

As described by Hae-Ji Lee et al. (2019), 1.0 g of fresh mice feces was diluted in 10 mL of Gifu Anaerobic Medium (GAM). The mixture was then centrifuged at 1500 rpm for 5 min, and the concentration of *B. breve* LE4 was adjusted to 1×10^9 CFU/mL through plate counting. This suspension was co-cultured anaerobically with eight *Bifidobacterium* strains, each at a concentration of 1×10^9 CFU/mL, in GAM broth at 37°C for 24 h. Following co-cultivation, the cultures were sonicated on ice for 1 hour, centrifuged at 1400 rpm for 10 minutes, and then sequentially filtered through 0.45 μm and 0.22 μm filters. The LPS concentration was subsequently measured using a Limulus Amebocyte Lysate (LAL) assay kit (Shanghai Enzyme-linked Biotechnology Co., Ltd., Shanghai, China).

2.4 Animals and Experimental Design

2.4.1 Animals

Thirteen male APP/PS1 transgenic mice (3 months old) and five age-matched wild-type (WT) littermates (B6C3 background) were obtained from Hangzhou Ziyuan Laboratory Animal Technology Co., Ltd. (Hangzhou, China). The mice were housed under specific-pathogen-free conditions, maintained at a temperature of 20–22°C with 55±5% humidity, and subjected to a 12-hour light/dark cycle, with ad libitum access to food and water. All procedures were approved by the Animal Ethics Committee of Jilin Agricultural University (No. 20240415001).All procedures were strictly conducted in accordance with the institutional Guidelines for Care and Use of Laboratory Animals.

2.4.2 Experimental Design

The animal flowchart of this study is shown in Fig. 1. A total of 15 APP/PS1 mice were randomly assigned to two groups (n = 5-8): the Alzheimer's Disease (AD) group, which received PBS gavage, and the experimental group, which received *B. breve* LE4 at a dosage of 1×10^9 CFU/mL per 10 g body weight per day. WT mice were also administered PBS gavage. After 12 weeks, fecal samples were collected and stored at −80°C. Following behavioral assessments, the mice were euthanized via CO_2 asphyxiation, and brain, colon, liver, and blood samples were collected for further analyses (Fig. S1).

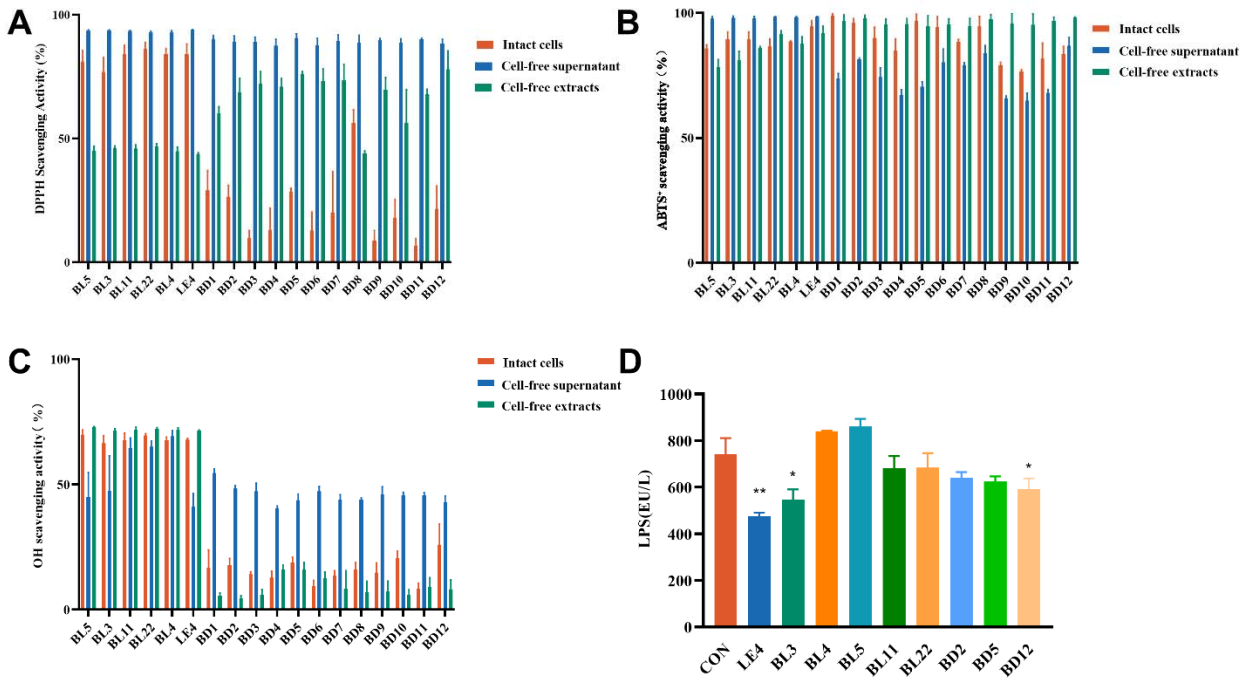

Fig. 1. *In vitro* evaluation of *Bifidobacterium* strains for antioxidant activity and suppression of gut microbiota-derived LPS production. (A-C) Radical scavenging capacity of *Bifidobacterium* intact cells, cell-free supernatants, and cell-free extracts against DPPH (A), ABTS (B), and hydroxyl (•OH) radicals (C). (D) Inhibitory effects on gut microbiota-derived LPS production. *$P < 0.05$ vs. CON group; **$P < 0.01$ vs. CON group.

2.5 Behavioral Experiments

2.5.1 Morris Water Maze (MWM) Experiment

Following 12 weeks of probiotic intervention, spatial memory performance was evaluated in all four experimental groups using the Morris Water Maze system (MWM; Chengdu Taimeng, WM-100). In accordance with the protocol established by Qian et al.[29], mice were first acclimatized to the testing environment for 24 h prior to commencing a five-day spatial navigation training protocol. During training sessions, each mice performed four daily trials to locate a submerged platform positioned in one of four quadrants, with each trial limited to 60 seconds (Xiao et al., 2023). On day 6, the platform was removed for the probe trial to evaluate spatial memory retention. Mice were introduced from the first quadrant, and their performance was assessed by measuring platform crossings, target zone duration, and total swimming distance during the 60-second observation period. Throughout both training and probe phases, mice movement trajectories were continuously recorded using an automated image acquisition and analysis system (Chengdu Taimeng, WMT-100) for comprehensive behavioral analysis.

2.5.2 Open Field Test (OFT) Experiment

Behavioral assessment was conducted using an open field apparatus (Chengdu Taimeng, OFT-100) featuring a 5×5 grid floor configuration. The central nine squares were designated as the central zone, with the remaining perimeter squares constituting the peripheral zone. Testing was performed under controlled conditions with reduced illumination and minimal ambient noise to limit external interference (O. B et al., 2020). Each mice was initially positioned at the center of the arena and permitted unrestricted exploration for 5 min. Key behavioral parameters, including rearing frequency, central zone occupancy duration, and total ambulatory distance, were automatically recorded by the tracking system. Between trials, the apparatus was thoroughly cleaned with 75% ethanol solution to remove potential olfactory cues and ensure testing consistency.

2.5.3 Nest Building Test (NBT)

After 48 hours of group housing, mice were transitioned to individual cages for adaptation. Each cage was prepared with a standardized 1-cm layer of corn cob bedding, supplemented with sterile cotton after 12 h. Nest construction quality was evaluated 18 h later using a validated four-point scoring system: 1, unmodified, scattered cotton; 2, loosely gathered cotton without nest structure; 3, partially formed flat nest; and 4, well-structured, compact nest with evident chewing marks.

2.6 Histological Analysis

Paraffin-embedded sections of the colon, liver, and brain were prepared for histological analysis. Liver sections were stained with hematoxylin and eosin (H&E). Brain tissues were embedded in paraffin and serially sectioned at 5 μm thickness. Sections underwent dewaxing and antigen retrieval, followed by blocking with 10% goat serum. Subsequently, sections were incubated with amyloid β (Aβ) primary antibody at 4°C overnight, followed by secondary antibody incubation at room temperature. After two washes with phosphate-buffered saline (PBS), sections were incubated with horseradish peroxidase-diaminobenzidine (HRP-DAB) chromogen and counterstained with hematoxylin. Sections were examined under an optical microscope, and Aβ-positive signals were quantified using ImageJ software.

For immunofluorescence analysis, brain sections were deparaffinized in xylene and blocked with 3% bovine serum albumin (BSA) to minimize nonspecific binding. Sections were incubated overnight at 4°C with antibodies against p-tau, Iba-1, GFAP, PSD95, SYNAPSIN I, Occludin, and ZO-1 (Servicebio, China), followed by incubation with FITC-conjugated CY3-labeled goat anti-rabbit IgG (Servicebio, China). Nuclei were counterstained with 4',6-diamidino-2-phenylindole (DAPI). Images were acquired using an inverted fluorescence microscope (Nikon, Tokyo, Japan), and fluorescence intensity was quantified with ImageJ software.

2.7 Biochemical Indicators Measurement

Serum triglyceride (TG) and total cholesterol (TC) levels were quantified using commercially available biochemical assay kits (Nanjing Jiancheng Bioengineering Institute, Nanjing, China) following the manufacturer's protocols.

2.8 ELISA Analysis of Inflammatory Cytokines and Neurobiochemical Markers

Brain and colon tissue homogenates were prepared in ice-cold PBS and centrifuged at 12,000 ×g for 10 min at 4°C to obtain the supernatant. Serum and tissue supernatants were subsequently analyzed using commercial ELISA kits (Shanghai Enzyme-linked Biotechnology Co., Ltd., China) following the manufacturer's instructions. The assay quantified the concentrations of interleukin (IL)-1β, IL-10, IL-17, IL-18, IL-22, amyloid beta peptides (Aβ1-40 and Aβ1-42), lipopolysaccharide (LPS), postsynaptic density protein 95 (PSD95), brain-derived neurotrophic factor (BDNF), NOD-like receptor family pyrin domain containing 3 (NLRP3), insulin (INS), and glucagon-like peptide-1 (GLP-1).

2.9 Western Blot Analysis

Brain and colon tissues were immediately harvested and homogenized in ice-cold lysis buffer using a tissue homogenizer (Ji et al., 2024; Zhang et al., 2023). Protein concentrations were quantified using an enhanced bicinchoninic acid (BCA) protein assay kit (Beyotime, China). Protein samples were denatured at 95°C for 5 min prior to electrophoresis. Protein separation was performed using sodium dodecyl sulfate-polyacrylamide gel electrophoresis (SDS-PAGE) with an initial voltage of 80 V for 30 min, followed by 120 V for 70 min. Subsequently, proteins were transferred to polyvinylidene fluoride (PVDF) membranes at 300 mA for 90 min. Membranes were blocked with 5% non-fat dry milk for 90 min at room temperature, followed by overnight incubation at 4°C with the following primary antibodies: p-Tau231 (1:1000, Wanleibio), Tau (1:1000, Wanleibio), SYNAPSIN I (1:1000, Santa Cruz), PSD-95 (1:1000, Santa Cruz), GFAP (1:1000, Santa Cruz), IBA-1 (1:1000, Abclonal), β-amyloid (1:1000, Santa Cruz), Occludin (1:1000, Bioworld), ZO-1 (1:1000, Wanleibio), ASC (1:1000, Abcam), pro-Caspase-1 p20 (1:1000, Bioworld), NLRP3 (1:1000, Proteintech), IL-1β (1:1000, Abcam), TLR4 (1:1000, Wanleibio), MyD88 (1:1000, Wanleibio), IKKα (1:1000, Wanleibio), p-NF-κB-p65 (1:2000, Abways), and NF-κB-p65 (1:2000, Abways). All antibodies were diluted according to the manufacturers' protocols. After primary antibody incubation, membranes were probed with horseradish peroxidase-conjugated secondary antibodies (1:20000, Absin) for 1 h at room temperature. Protein bands were visualized using enhanced chemiluminescence detection reagents and quantified using ImageJ software. β-actin (1:20000, Proteintech) served as the internal loading control for data normalization.

2.10 Fecal Microbiota DNA Extraction and 16S rRNA Gene Sequencing Analysis

Total genomic DNA was aseptically extracted from the cecal contents of aged mice. The hypervariable V3-V4 regions of bacterial 16S rRNA genes were amplified using universal primers 341F (5'-CCTAYGGGRBGCASCAG-3') and 806R (5'-GGACTACNNGGGTATCTAAT-3'). PCR amplicons were subjected to paired-end sequencing (2×250 bp) on an Illumina MiSeq platform at Shanghai Personal

Biotechnology Co., Ltd (Shanghai, China). Raw sequencing reads were processed into amplicon sequence variants (ASVs) using the DADA2 pipeline. Beta-diversity analysis was performed through principal coordinates analysis (PCoA) based on Jaccard distance metrics, implemented in QIIME2's q2-diversity module with visualization in Emperor at Shanghai Personal Biotechnology Co., Ltd (Shanghai, China). Functional profiling of microbial communities was predicted using PICRUSt2 (Phylogenetic Investigation of Communities by Reconstruction of Unobserved States) with reference to both MetaCyc (https://metacyc.org/) and KEGG (https://www.kegg.jp/) metabolic pathway databases.

2.11 Short-chain Fatty Acids (SCFAs) Analysis

Approximately 40 mg of feces was homogenized in 500 μL of saturated sodium chloride, incubated for 30 minutes, and maintained on ice throughout the processing. Samples were acidified with 20 μL of sulfuric acid and extracted with 800 μL of ether, followed by centrifugation (12,000 × g, 15 min, 4°C). The supernatants were purified using anhydrous sodium sulfate and analyzed by gas chromatography-mass spectrometry (GC-MS). SCFAs (acetate, propionate, butyrate, isobutyrate, isovalerate, and hexanoic acid) were quantified using an Agilent 8890 GC system equipped with an HP-INNOWAX column. The injection volume was 1 μL with a split ratio of 10:1 and a carrier gas flow rate of 1 mL/min (Caetano-Silva et al., 2023). The injector and detector temperatures were maintained at 250°C. The column temperature program was as follows: initial temperature 60°C (3 min), ramped to 190°C at 3.5°C/min, then increased to 230°C at 25°C/min, and held for 3 min. Quantification was performed using external calibration standards. All experimental procedures in this study were performed at Suzhou PANOMIX Biomedical Tech (Suzhou, China).

2.12 Untargeted Metabolomics Analysis

Fecal metabolomic profiling was conducted using a Vanquish UHPLC system (Thermo Fisher Scientific) equipped with an ACQUITY UPLC® HSS T3 column (2.1 × 100 mm, 1.8 μm; Waters). The chromatographic conditions were as follows: flow rate 0.3 mL/min, injection volume 2 μL, and column temperature maintained at 40°C. For LC-ESI(+)-MS analysis, the mobile phases consisted of 0.1% formic acid in water (A2) and acetonitrile (B2), while LC-ESI(-)-MS employed 5 mM ammonium formate (A3) and acetonitrile (B3). Both analyses used identical gradient programs: 8%–98% B over 8 min, held at 98% B for 2 min, followed by column re-equilibration (Li et al., 2021; Imran et al., 2023). Mass spectrometric detection was performed using a Q Exactive instrument operating in Full MS-ddMS2 mode. Full scan MS1 spectra were acquired over m/z 100–1000 at 70,000 resolution, while MS/MS spectra were collected at 17,500 resolution with a normalized collision energy of 30 eV. The spray voltages were set at 3.50 kV (ESI+) and -2.50 kV (ESI-), with the capillary temperature maintained at 325°C. Metabolite identification was performed by matching experimental masses against the HMDB, METLIN, MassBank, LipidMaps, mzCloud, and PANOMIX metabolomics databases, allowing for a mass error tolerance of 30 ppm. All experimental procedures in this study were performed at Suzhou PANOMIX Biomedical Tech (Suzhou, China).

2.13 Statistical Analyses

All experimental data are presented as mean ± standard deviation (SD). Statistical analyses and graph generation were performed using GraphPad Prism 8.0 (GraphPad Software Inc., San Diego, CA, USA) and R software (version 4.2.1). For comparisons between two groups, Student's t-test was used for normally distributed data, whereas the Mann-Whitney U test was employed for non-normally distributed data. ELISA data and behavioral data from the MWM, OFT, and NBT were analyzed using repeated-measures ANOVA or Kruskal-Wallis tests, depending on data distribution. Statistical significance was defined as $P < 0.05$ (*), with highly significant differences marked at $P < 0.01$ (**).

Western blot data were quantified using ImageJ or microplate reader software, respectively, and normalized to appropriate internal controls. Group comparisons were performed using t-tests or ANOVA with post hoc analysis, as described.

Microbiome sequencing data were processed into amplicon sequence variants (ASVs), and alpha and beta diversity indices were calculated using QIIME2. Principal coordinates analysis (PCoA) based on Jaccard distance was performed to evaluate differences in microbial community composition, with visualization conducted using Emperor.

Short-chain fatty acid (SCFA) levels were analyzed by gas chromatography-mass spectrometry (GC-MS), with quantification based on external standard calibration curves. Metabolomic data from mice fecal samples were analyzed using Compound Discoverer software (Thermo Fisher Scientific). Metabolite identification was achieved through database comparisons (HMDB, METLIN, mzCloud, and LipidMaps), excluding compounds exhibiting a relative standard deviation (RSD) >30%. Multivariate analyses, including principal component analysis (PCA) and orthogonal partial least squares discriminant analysis (OPLS-DA), were employed to identify metabolic profile patterns. Differential metabolites were determined using variable importance in projection (VIP) values > 1.0 and $P < 0.05$

3. Result

3.1 Screening of Infant-Derived Bifidobacterium Strains for In Vitro Antioxidant Properties

The *in vitro* antioxidant capacities of eighteen infant-derived *Bifidobacterium* strains were systematically evaluated through intact-cell, cell-free supernatant, and cell-free extract assays (Fig. 1A-C). Among intact cells, *B. longum* strains BL3 (76.93 ± 5.99%), BL4 (84.12 ± 2.29%), BL5 (81.10 ± 4.45%), BL11 (84.17 ± 3.58%), BL22 (86.26 ± 2.63%), and *B. brevis* strain LE4 (84.26 ± 3.94%) exhibited significant DPPH• scavenging activity (Table S1). Notably, the cell-free supernatant of *B. brevis* LE4 demonstrated the highest DPPH• scavenging capacity (94.09 ± 0.03%), while the cell-free extract of *B. animalis* strain BD12 showed substantial activity (78.08 ± 7.37[a]). In the ABTS• scavenging assay, intact cells of *B. animalis* strains BD1 (99.02 ± 0.87%) and BD5 (96.79 ± 2.74%) displayed the strongest scavenging activity, although other strains also exhibited considerable efficacy (Table S2). The cell-free supernatants of BL3 (98.06 ± 0.68%), BL4 (98.42 ± 0.16%), BL5 (97.81 ± 0.84%), BL11 (97.96 ± 0.68%), BL22 (98.50 ± 0.20%), and LE4 (98.50 ± 0.17%) showed robust ABTS•+ scavenging activity. Regarding cell-free extracts, *B. animalis* strains BD2 (97.86 ± 1.26%) and BD12 (98.29 ± 0.15%) exhibited the highest ABTS•+ scavenging capacity. In the

hydroxyl radical (•OH) assay (Table S3), both intact cells and cell-free extracts of BL3 (66.39 ± 3.17%; 71.57 ± 0.72%), BL4 (67.70 ± 1.26%; 71.88 ± 0.78%), BL5 (69.85 ± 1.96%; 72.80 ± 0.31%), BL11 (67.74 ± 2.80%; 71.94 ± 0.95%), BL22 (69.56 ± 0.71%; 72.23 ± 0.46%), and LE4 (67.89 ± 0.63%; 71.55 ± 0.22%) demonstrated significant •OH scavenging activity, whereas their supernatants showed negligible effects.

Based on comprehensive antioxidant profiles across DPPH•, ABTS•+, and •OH assays, strains exhibiting statistically significant effects in at least two of the three free-radical scavenging assays were selected for further investigation. Consequently, strains BL3, BL4, BL5, BL11, BL22, LE4, and BD12 were chosen for subsequent evaluation of their inhibitory effects on lipopolysaccharide (LPS) production in fecal microbiota cultures.

3.2 Antioxidant Bifidobacterium Effectively Inhibits Lipopolysaccharide Production in Fecal Microbiota Cultures

We evaluated the inhibitory effects of seven antioxidant-active *Bifidobacterium* strains on lipopolysaccharide (LPS) production by intestinal microbiota (Fig. 1D). Compared with the control group, BL4 (13.46%) and BL5 (16.31%) significantly increased LPS levels in intestinal flora, whereas the other five *Bifidobacterium* strains exhibited significant inhibition. Among these, LE4 (35.62%), BL3 (26.21%), and BD12 (20.04%) demonstrated particularly strong inhibitory effects, with LE4 showing the most pronounced suppression (**$P < 0.01$). Consequently, *B. breve* LE4 was selected for subsequent in vivo assessment.

3.3 B. breve LE4 Ameliorates Learning and Memory Deficits in the APP/PS1 Mice Model

To evaluate the therapeutic potential of *B. breve* LE4 in APP/PS1 transgenic mice, animals received daily gavage for 12 weeks, followed by behavioral testing using the Morris water maze, open field test, and nest nest-building test. These tests measured cognitive performance, anxiety-like behaviors, and daily living activities, providing comprehensive insight into *B. breve* LE4's efficacy against disease progression. Notably, *B. breve* LE4-treated mice exhibited significantly shorter escape latencies than wild-type controls from day one (Fig. 2A, C) ($P < 0.01$). In the probe trial, *B. breve* LE4-treated mice crossed the former platform site more often than controls, indicating improved memory retention. Following *B. breve* LE4 treatment, mice showed increased rearing frequency and more central-zone activity, indicative of enhanced exploration and reduced anxiety (Fig. 2B, D). Nest-building—reflecting daily living skills and motivation—was impaired in AD mice, with partial nests at 24 h and disrupted nests at 48 h (Fig. 2E). *B. breve* LE4 administration significantly improved nest-building, yielding fully formed nests by 24 h. Together, these results demonstrate that *B. breve* LE4 intervention ameliorates behavioral deficits in the AD mice model.

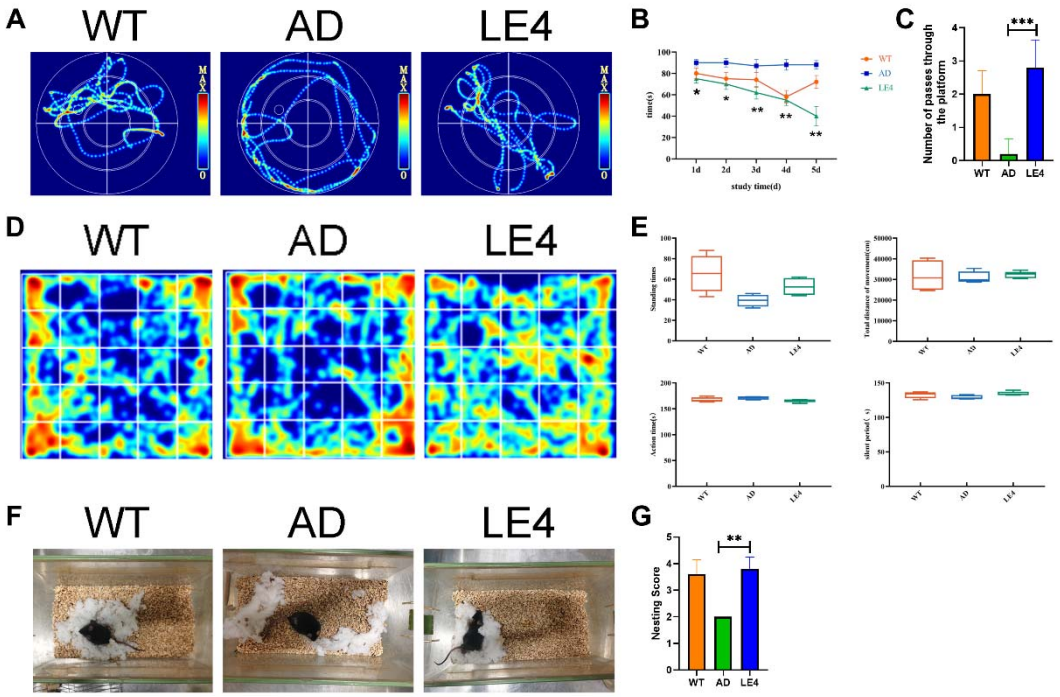

Fig. 2. Behavioral test results in APP/PS1 mice. (A) Latency to reach the platform during five days of Morris water maze training. (B) Total movement time in the open field test. (C) Representative swimming trajectories on day 6 in the Morris water maze. (D) Representative movement trajectories in the open field test. (E) Representative nesting behavior images at 0, 24, and 48 hours. *Significance: *$P < 0.05$ compared with the WT group, **$P < 0.01$ compared with the AD group.

3.4 B. breve LE4 Alleviates Histopathological Alterations in the Brain, Colon, and Liver of APP/PS1 Transgenic Mice

3.4.1 Histopathological Analysis of Mice Liver

Hematoxylin and eosin (H&E) staining revealed structural abnormalities in the liver tissues of APP/PS1 mice. Characterized by focal macrophage clustering, hepatocellular inflammatory infiltration, and enlarged intracellular lipid droplets. *B. breve* LE4 administration mitigated hepatic inflammation and restored lipid droplet morphology (Fig. 3A).

3.4.2 Histopathological Assessment of Murine Brain Tissue

In APP/PS1 mice, the hippocampus, essential for learning and memory, is particularly vulnerable to early AD pathology, often manifesting as spatial learning and memory impairments. The intervention effect on *B. breve* LE4 can be demonstrated by evaluating the pathological indices of the hippocampus.

Immunohistochemistry revealed that Aβ plaque deposition in the brains of APP/PS1 (AD) mice was significantly greater than in WT controls ($P < 0.05$; Fig.3B,H) and was markedly reduced following *B. breve* LE4 treatment ($P < 0.05$). Western blot analysis corroborated these findings, showing elevated hippocampal Aβ levels in AD mice that were significantly attenuated by *B. breve* LE4 intervention ($P < 0.05$; Fig. 3H). Immunofluorescence demonstrated increased aggregation of phosphorylated tau (p-tau), along with upregulated expression of the microglial marker IBA-1 and astrocytic marker GFAP in AD brains compared to WT (Fig. 3E–G, I), all of which were significantly diminished after *B. breve* LE4 administration. Western blotting confirmed the downregulation of p-tau, IBA-1, and GFAP in the hippocampus of *B. breve*

LE4-treated mice ($P < 0.05$; Fig. 3I, J). Collectively, these results indicate that *B. breve* LE4 reduces p-tau aggregation and inhibits glial activation, thereby conferring neuroprotection and alleviating cognitive deficits in APP/PS1 mice.

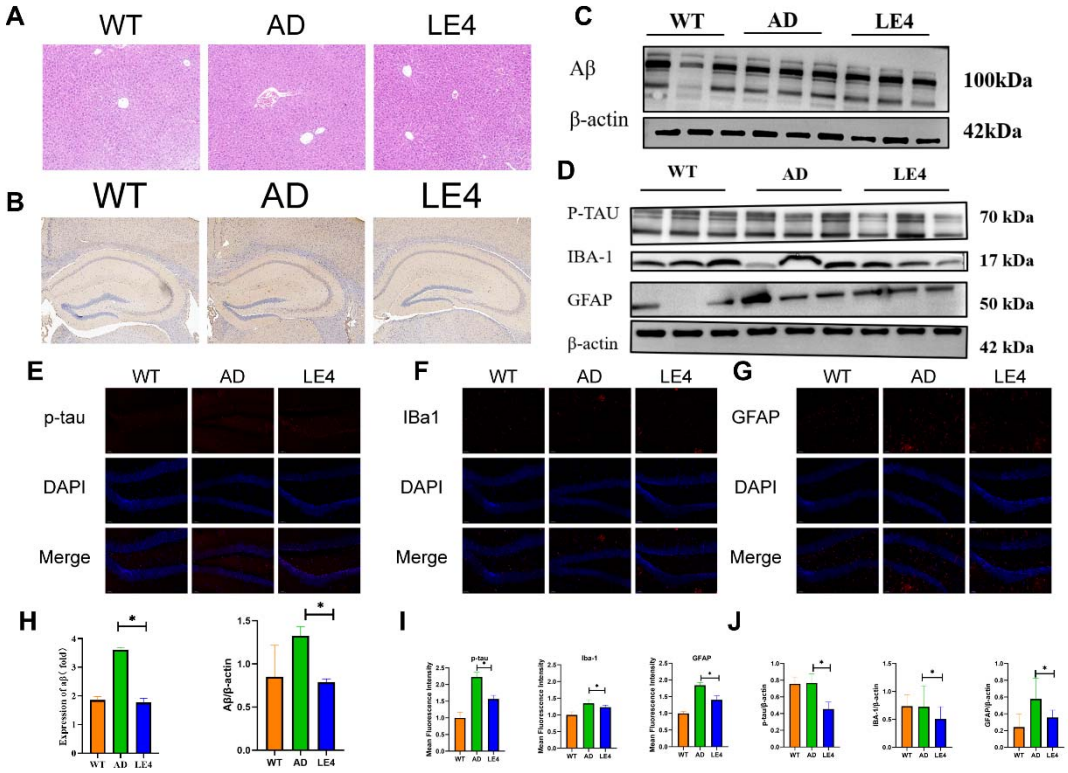

Fig. 3. *B. breve* LE4 Modulates Alzheimer's Pathology in APP/PS1 Mice. (A) Representative hematoxylin and eosin (HE) stained liver sections from mice. (B) Representative immunohistochemical images of amyloid-β (Aβ) plaques in the hippocampus of WT, AD, and *B. breve* LE4-treated APP/PS1 mice. (C) Western blot analysis of hippocampal Aβ and β-actin (loading control). (D)Western blot analysis of p-tau, Iba-1, and GFAP expression in the hippocampus. (E–G) Immunofluorescence staining of phosphorylated tau (p-tau), microglia (Iba-1), and astrocytes (GFAP) in hippocampal sections. (H) Quantification of Aβ plaque burden using ImageJ. Densitometric quantification of Aβ levels normalized to β-actin using ImageJ. **(**I) ImageJ quantification of immunofluorescence intensity for p-tau, Iba-1, and GFAP. (J) Densitometric quantification of p-tau, Iba-1, and GFAP bands normalized to β-actin using ImageJ. Significance: *$P < 0.05$ compared with the AD group.

3.4.3 Evaluation of Synaptic Function in Mice Brain Tissue

Immunofluorescence analysis revealed that APP/PS1 (AD) mice exhibited significantly elevated hippocampal expression of the presynaptic protein Synapsin I and the postsynaptic density protein PSD-95 compared to the WT group, likely reflecting a compensatory response to early synaptic pathology (Fig. 4A, B). Following *B. breve* LE4 treatment, Synapsin I and PSD-95 levels were further increased. These observations were confirmed by Western blotting (Fig. 4C, D), which demonstrated a significant upregulation of PSD-95 in the *B. breve* LE4-treated group ($P < 0.05$). Collectively, these data indicate that *B. breve* LE4 enhances both presynaptic and postsynaptic membrane function, thereby mitigating synaptic dysfunction in APP/PS1 mice.

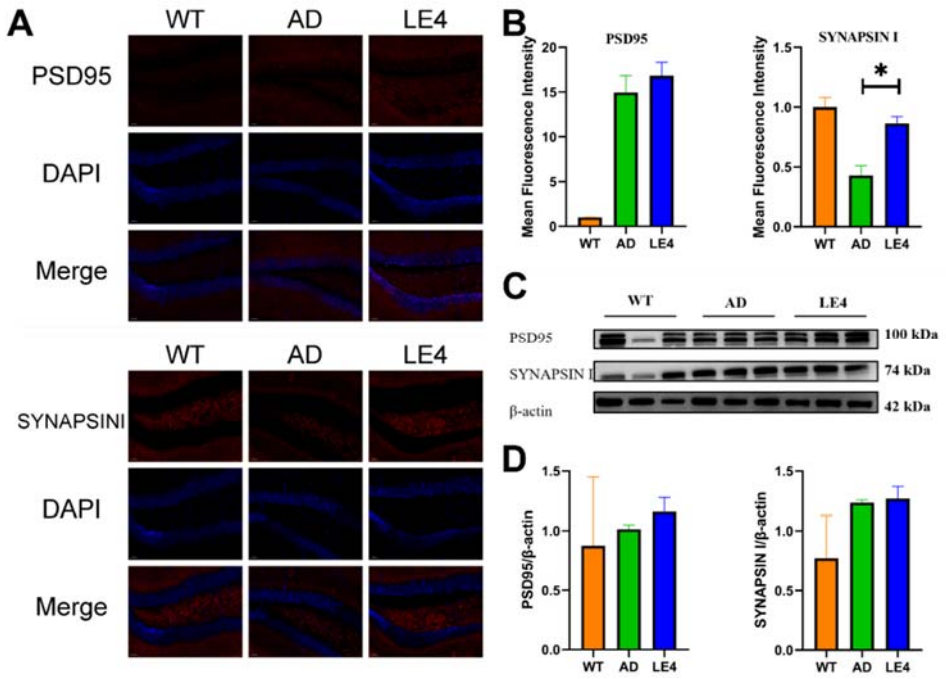

Fig. 4. *B. breve* LE4 enhances synaptic plasticity in APP/PS1 mice. (A) Immunofluorescence staining of PSD-95 and Synapsin I. (B) Quantification of PSD-95 and Synapsin I immunofluorescence intensity. (C) Western blot analysis of PSD-95 and Synapsin I. (D) Quantitative analysis of western blot bands. *Significance: $*P < 0.05$ compared with the AD group.

3.4.4 Functional evaluation of colon tight junction protein

Immunofluorescence analysis of colonic tissue revealed a significant reduction in ZO-1 and occludin fluorescence intensity in APP/PS1 (AD) mice compared to WT controls ($P < 0.05$; Fig. 5A, B). *B. breve* LE4 treatment markedly restored ZO-1 and occludin expression, yielding a clear, continuous, and well-organized staining pattern. Western blotting (Fig. 5C, D) confirmed the upregulation of these tight junction proteins following *B. breve* LE4 administration ($P < 0.05$). Together, these results indicate that *B. breve* LE4 enhances intestinal barrier integrity in APP/PS1 mice by restoring tight junction protein expression.

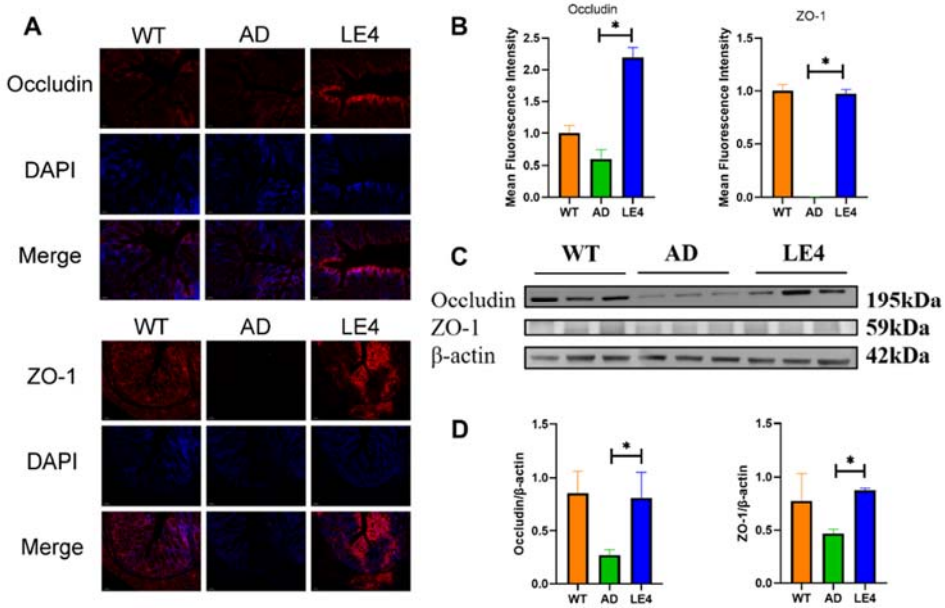

Fig. 5. LE4 restores intestinal barrier function in APP/PS1 mice. (A) Immunofluorescence staining of tight junction proteins ZO-1 and Occludin. (B) Quantification of ZO-1 and Occludin fluorescence intensity. (C) Western blot analysis of ZO-1 and Occludin. (D) Quantitative analysis of Western blot bands. *Significance: $*P < 0.05$ compared with the AD group.

3.5 Comprehensive Evaluation of Metabolic Parameters, Neuroinflammation, and Enterogenous Endotoxin in Mice

To evaluate the effects of *B. breve* LE4 on cognitive function and systemic physiology, APP/PS1 mice were orally administered *B. breve* LE4 daily for 12 weeks. Body weight and food intake were recorded weekly (Fig. 6A, B). Although there was no significant difference in food intake between groups, the *B. breve* LE4-treated group exhibited significantly reduced body weight compared to the AD group during weeks 3 to 10 ($P < 0.05$). The liver index was markedly elevated in AD mice (Fig. 6E), but significantly decreased following *B. breve* LE4 treatment, returning to levels comparable to WT mice ($P < 0.01$). Given the increased water intake observed in AD mice, fasting blood glucose and 2-hour postprandial glucose levels were measured. While fasting glucose in the AD group remained within the normal range (4.5–8.1 mmol/L), both fasting and postprandial blood glucose levels were elevated compared to the WT group. *B. breve* LE4 intervention effectively restored glucose levels to those observed in WT mice, suggesting that *B. breve* LE4 may modulate glucose metabolism (Fig. 6C, D).

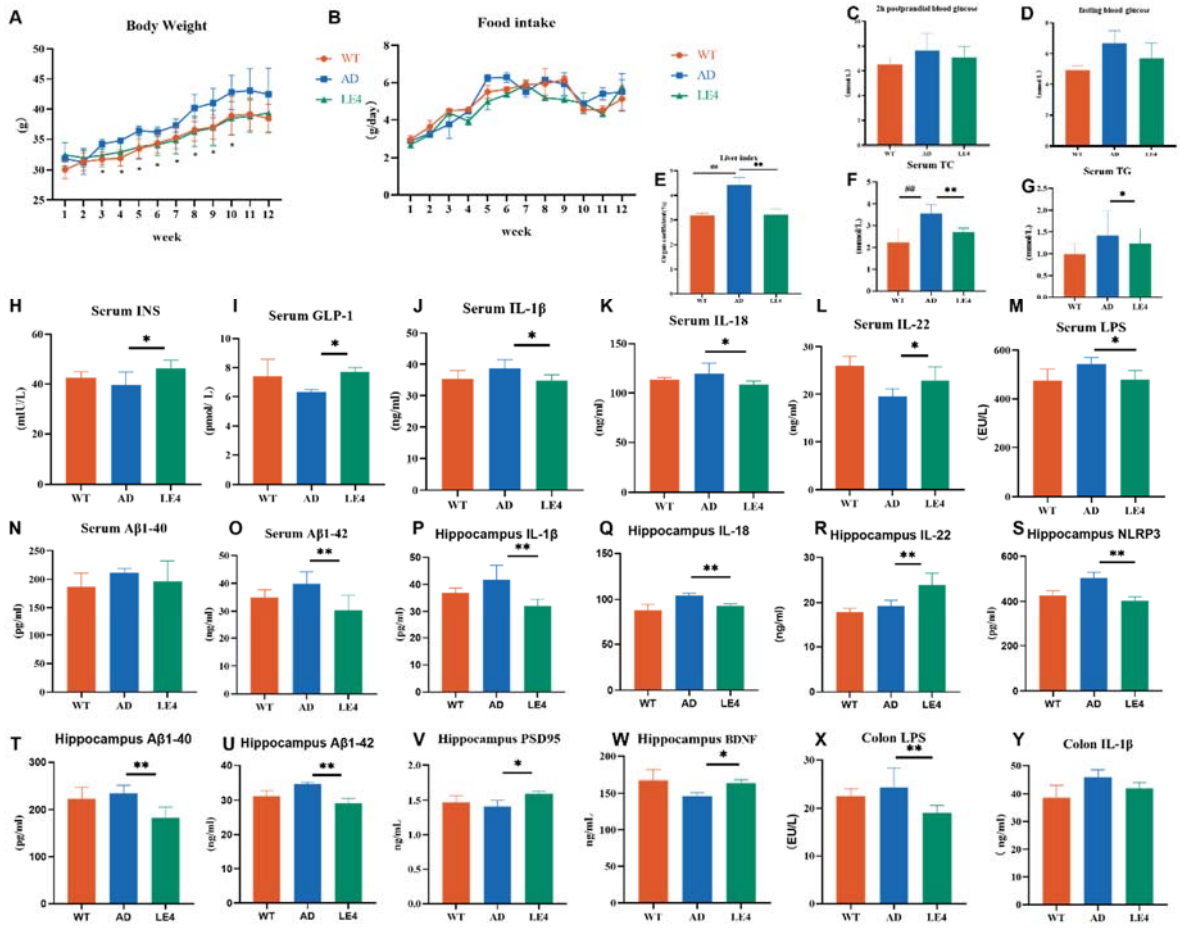

Fig. 6. Comprehensive evaluation of metabolic indicators, neuroinflammation, and gut-derived endotoxins in APP/PS1 mice treated with *B. breve* LE4. (A) Body weight changes over 12 weeks. (B) Weekly food intake. (C, D) Fasting blood glucose and 2-hour postprandial blood glucose levels. (E) Liver index. (F–I) Serum levels of total cholesterol (TC), triglycerides (TG), insulin (INS), and glucagon-like peptide-1 (GLP-1). (J–L) Serum levels of pro-inflammatory cytokines IL-1β and IL-18, and anti-inflammatory cytokine IL-22. (M) Serum lipopolysaccharide (LPS) levels. (N, O) Serum concentrations of Aβ1-40 and Aβ1-42. (P–S) Hippocampal expression of IL-1β, IL-18, IL-22, and NLRP3 inflammasome. (T, U) Hippocampal levels of Aβ1-40 and Aβ1-42. (V, W) Expression of synaptic plasticity markers PSD95 and BDNF in the hippocampus. (X, Y) Expression of LPS and IL-1β in colon tissue. Data are presented as mean ± SEM. *$P < 0.05$, **$P < 0.01$ compared with AD group.

Serum glucose and lipid metabolism markers were further assessed (Fig. 6F-I). Total cholesterol (TC) and triglyceride (TG) levels were significantly elevated in the AD group but were substantially reduced by *B. breve* LE4 treatment. Additionally, serum insulin (INS) and glucagon-like peptide-1 (GLP-1), both of which were decreased in the AD group, were significantly increased following *B. breve* LE4 administration, consistent with the observed improvements in weight and glycemic control.

AD mice also exhibited pronounced neuroinflammation (Fig. 6J-O), reflected by elevated serum levels of proinflammatory cytokines IL-1β and IL-18, both of which were significantly reduced in the *B. breve* LE4 group. Although IL-10 levels remained unchanged across groups, IL-22 was significantly decreased in AD mice and restored following *B. breve* LE4 treatment. Notably, serum levels of lipopolysaccharide (LPS) were significantly higher in the AD group, but were markedly reduced after *B. breve* LE4 intervention ($P < 0.05$). Furthermore, serum concentrations of Aβ1-40 and Aβ1-42 were increased in AD mice, but decreased with *B. breve* LE4 treatment, with Aβ1-42 showing a significant reduction.

Neuroinflammatory markers in brain tissue were also evaluated (Fig. 6P-U). The expression of IL-1β, IL-18, and NLRP3 inflammasome components was significantly higher in the AD group and notably suppressed in the *B. breve* LE4-treated mice ($P < 0.05$), while IL-22 expression was significantly upregulated after *B. breve* LE4 intervention. These changes indicate that *B. breve* LE4 attenuates AD-related neuroinflammation by decreasing pro-inflammatory cytokines and enhancing anti-inflammatory responses.

Synaptic plasticity was assessed by evaluating the expression of brain-derived neurotrophic factor (BDNF) and postsynaptic density protein 95 (PSD95) (Fig. 6V-W). Both markers were significantly elevated in the *B. breve* LE4 group compared to AD controls ($P < 0.05$), consistent with the observed behavioral improvements and suggesting enhanced synaptic function.

Considering the elevated serum LPS levels in AD mice, colonic expression of LPS and IL-1β was examined (Fig. 6X-Y). *B. breve* LE4 treatment significantly reduced both LPS levels ($P < 0.05$) and IL-1β expression in the colon. These findings, in conjunction with previous immunofluorescence data showing restored tight junction protein expression, support the hypothesis that increased LPS in AD may contribute to intestinal barrier disruption, which can be ameliorated by *B. breve* LE4 intervention.

3.6 B. breve LE4 Modulates Gut Microbiota Composition in APP/PS1 Mice

Gut microbiota composition was profiled by 16S rRNA gene sequencing. As shown in Fig. 7A, α-diversity metrics—including Chao1, Shannon, Simpson, and Observed_species—were calculated to assess microbial diversity. All four indices were significantly reduced in AD mice, indicating a loss of microbial diversity, which was partially restored following *B. breve* LE4 treatment. Venn diagram analysis (Fig. 7 B) revealed 2099, 508, and 1646 unique OTUs/ASVs in WT, AD, and *B. breve* LE4 groups, respectively, with 372 OTUs/ASVs shared across all groups. This finding suggests that *B. breve* LE4 increases microbial richness in APP/PS1 mice. Principal Coordinates Analysis (PCoA; Fig. 7C) showed distinct clustering of AD samples away from WT, while *B. breve* LE4-treated samples overlapped partially with WT, indicating that *B. breve* LE4 partially restores microbial community structure.

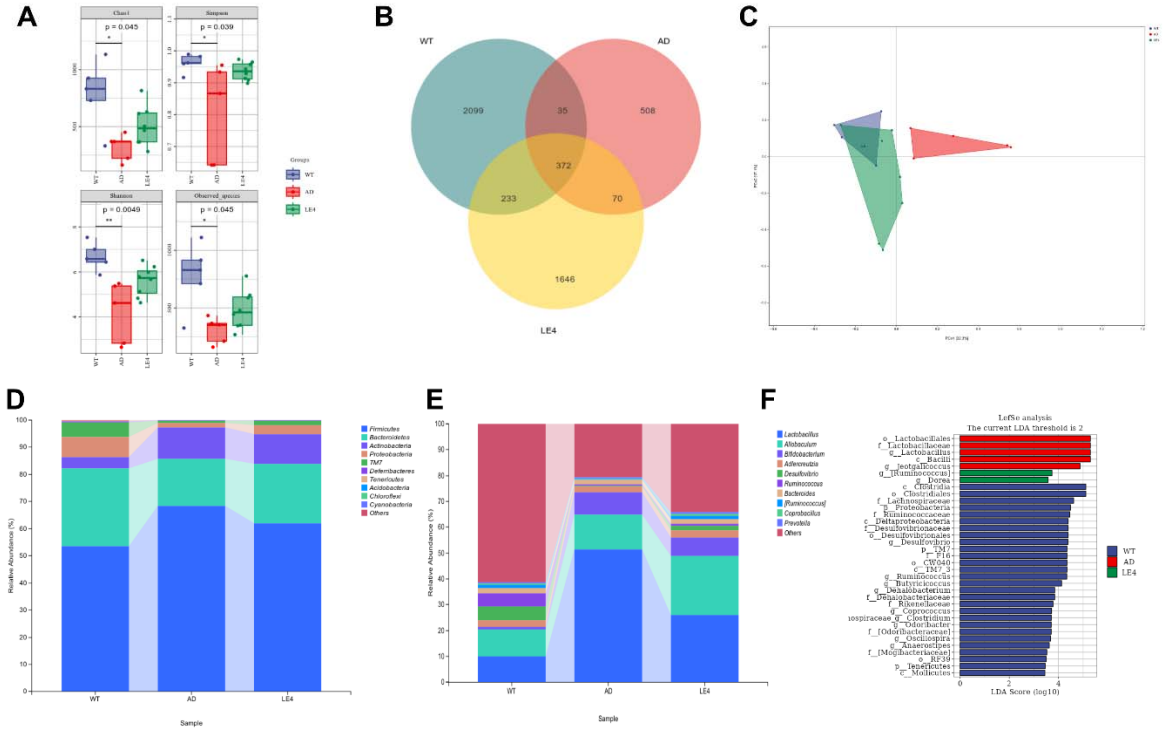

Fig. 7 *B. breve* LE4 restores gut microbiota diversity in APP/PS1 mice. (A) α-diversity indices, including Chao1, Shannon, Simpson, and Observed_species, showing a significant reduction in the AD group and restoration following *B. breve* LE4 treatment (*$P < 0.05$). (B) Venn diagram illustrating the number of unique and shared OTUs/ASVs among WT, AD, and *B. breve* LE4 groups. (C) Principal Coordinate Analysis (PCoA) based on unweighted UniFrac distances reveals distinct clustering of microbial communities, with partial overlap between WT and *B. breve* LE4 groups. (D) Taxonomic composition of gut microbiota at the phylum level. (E) Top 10 genera in relative abundance among groups at the genus level. (F) Histogram of LDA (Linear Discriminant Analysis) scores showing differentially abundant taxa among groups (LDA > 2, *$P < 0.05$).

Taxonomic bar plots at both the phylum and genus levels illustrated marked compositional differences among the three groups (Fig. 7D, E). At the phylum level, Clostridia abundance increased from 53.6% in WT to 68.4% in AD mice, whereas Bacteroidetes decreased, leading to an elevated Bacteroidetes/Clostridia ratio (from 1.86 to 3.98). *B. breve* LE4 treatment reduced Clostridia (to 62.03%) and increased Bacteroidetes (to 21.95%), adjusting the ratio to 2.83. Genus-level analysis showed elevated levels of *Lactobacillus*, *Bifidobacterium*, and *Prevotella* in AD mice, alongside reduced levels of *Allobaculum*, *Adlercreutzia*, Desulfovibrio, *Ruminococcus*, *Bacteroides*, and *Coprobacillus*.*B. breve* LE4 administration significantly decreased *Lactobacillus* and partially restored other genera toward WT levels.

Differential taxa were identified by LEfSe (LDA score > 2), highlighting AD-enriched microbial groups such as *Lactobacillus*, *Bacilli*, and *Jeotgalicoccus*, which may serve as potential microbial biomarkers(Fig. 7F). Conversely, *B. breve* LE4 treatment depleted these taxa and significantly enriched *Ruminococcus* and *Dorea*. Together, these results indicate that *B. breve* LE4 modulates the gut microbiota composition of APP/PS1 mice and may help restore microbial homeostasis disrupted in Alzheimer's disease pathology.

3.7 PICURSt Function Prediction of Gut Microbial Genes in APP/PS1 Mice

To investigate the functional potential of gut microbiota, microbial gene profiles were predicted based on the MetaCyc and KEGG databases (Fig. 8A, B). MetaCyc pathway analysis indicated enrichment in

categories such as biosynthesis, degradation/utilization/assimilation, detoxification, generation of precursor metabolites and energy, glycan pathways, macromolecular modification, and metal cluster-related metabolism. KEGG analysis revealed that metabolic pathways such as Cellular Processes, Environmental Information Processing, Genetic Information Processing, Human Diseases, Metabolism, and Organismal Systems were enriched, with metabolism-related genes accounting for approximately 60% of the total. Notably, the gene counts involved in lipid metabolism and glycan biosynthesis were comparable. Comparative analysis of differential metabolic pathways between groups revealed significant functional shifts (Fig. 8C). Notably, several pathways, including ECASYN-PWY (ornithine degradation pathway), were significantly altered in the *B. breve* LE4 group compared to the AD group. These findings suggest that *B. breve* LE4 intervention reshapes the metabolic potential of the intestinal microbiota, potentially contributing to its beneficial effects on host physiology and Alzheimer's disease pathology.

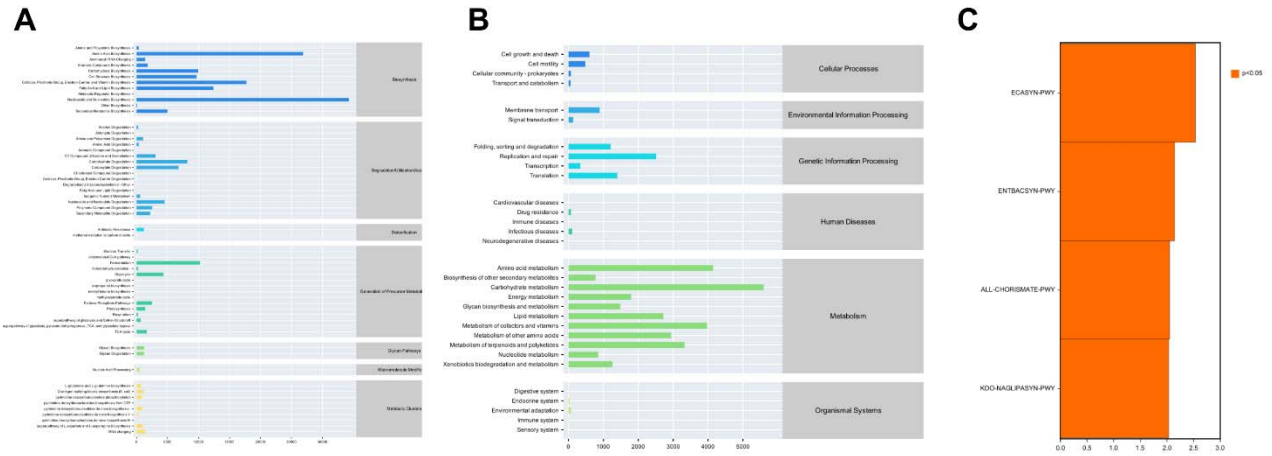

Fig. 8. Functional prediction of gut microbiota metabolic pathways. (A) Predicted MetaCyc pathways in gut microbiota of WT, AD, and *B. breve* LE4 groups. (B) KEGG level 2 functional category abundance across groups. (C) Differential MetaCyc metabolic pathways between the AD and *B. breve* LE4 groups, with significant enrichment highlighted.

3.8 B. breve LE4 restores SCFAs levels and modulates propionate, carbohydrate, and protein metabolism in APP/PS1 mice.

Fecal short-chain fatty acid (SCFA) levels were assessed across the three experimental groups. *B. breve* LE4 administration markedly increased fecal SCFA levels in APP/PS1 mice (Fig. 9A, B), with acetic acid, propionic acid, and butyric acid levels rising by 2.06-, 2.55-, and 4.15-fold, respectively ($P<0.001$, $P<0.05$, and $P<0.01$). Other SCFAs also exhibited an upward trend, although these changes were not statistically significant. These results suggest that *B. breve* LE4 supplementation can alleviate SCFAs dysregulation in APP/PS1 mice. KEGG pathway analysis revealed that (Fig.9C, D), compared to the AD group, WT mice harbored more metabolites associated with propionate metabolism, as well as carbohydrate and protein digestion and absorption. Compared with the *B. breve* LE4 group, AD mice exhibited reduced levels of metabolites associated with these pathways, suggesting that *B. breve* LE4 may mitigate AD pathology by modulating propionate, carbohydrate, and protein metabolism.

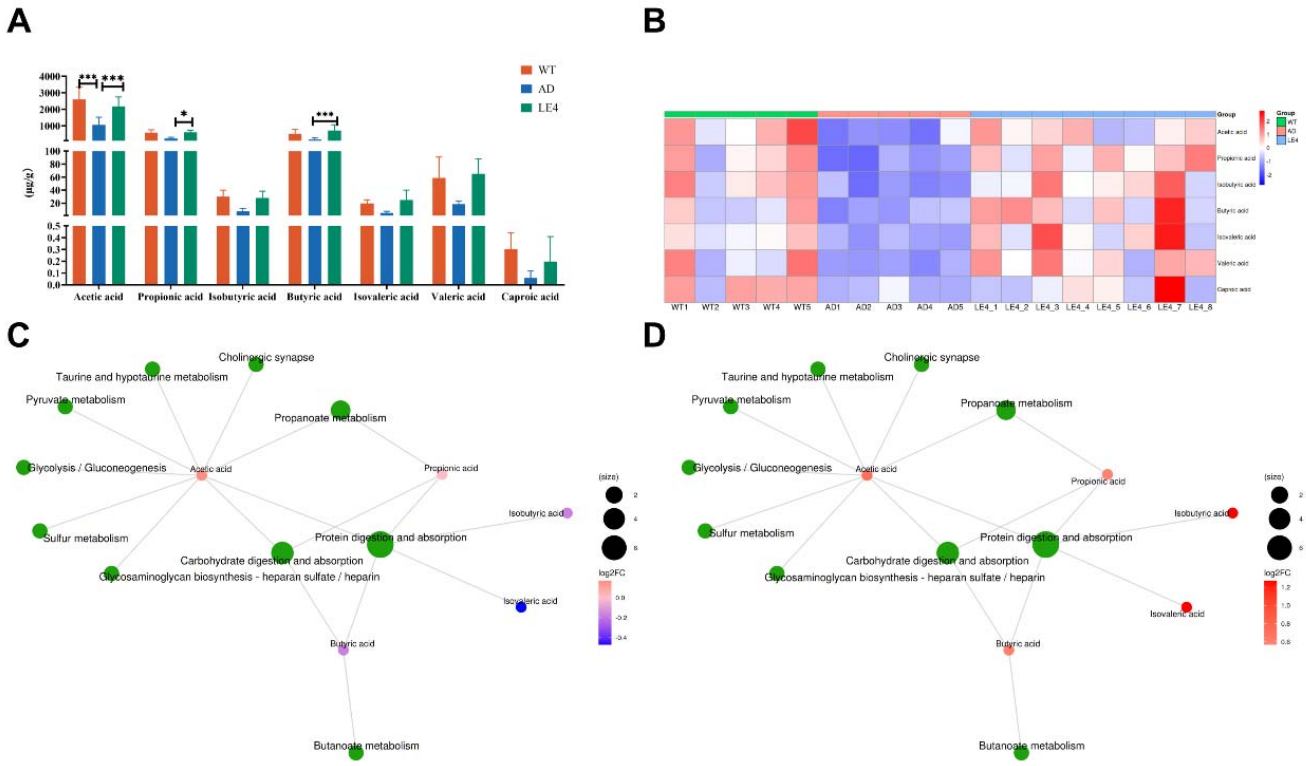

Fig. 9. Differential SCFA Metabolism and Associated Pathways in APP/PS1 Mice with *B. breve* LE4 Intervention. (A) Concentrations of seven short-chain fatty acids (SCFAs). (B) Heatmap showing the clustering of total SCFA metabolites, highlighting differential metabolites (VIP > 1, $p < 0.05$). (C, D) KEGG metabolic pathway analysis between WT and AD groups (C), and between AD and *B. breve* LE4 groups (D). In panels (C) and (D), green dots represent metabolic pathways, while colored dots denote metabolite molecules. The size of each pathway dot reflects the number of associated metabolites. The color gradient indicates the $\log_2$ fold change (FC) values of metabolites. (*$P< 0.05$, **$P< 0.01$, ***$P < 0.001$.)

3.9 B. breve LE4 Modulates Fecal Metabolomic Profiles in APP/PS1 Mice

To elucidate the modulatory effects of *B. breve* LE4 on intestinal metabolites, we performed non-targeted metabolomics analysis of fecal samples from experimental mice. As illustrated in Fig. 10A and 10B, multivariate statistical analyses, particularly partial least squares discriminant analysis (PLS-DA), demonstrated distinct clustering patterns among treatment groups. Our investigation specifically examined the influence of *B. breve* LE4 administration on fecal metabolite profiles in APP/PS1 mice, with significant metabolic differences observed between the AD model and *B. breve* LE4 intervention groups. Following exclusion of unannotated metabolites absent from both HMDB and KEGG databases, we identified 14 metabolites exhibiting significant alterations between these groups (Table 1 lists the fecal metabolites that showed significant differences between the AD and *B. breve* LE4-treated groups). The volcano plot revealed a significant upregulation of 24(S),25-epoxycholesterol, alpha-hydroxy-N-desmethyltamoxifen, and N-acetylglucosamine_N-acetylgalactosamine, as well as a marked downregulation of N-acetylcitrulline and arginine (Fig. 10C). KEGG pathway enrichment analysis revealed significant alterations in metabolic pathways including amino acid biosynthesis (arginine, proline, phenylalanine, tyrosine, and tryptophan), steroid hormone biosynthesis, the mTOR signaling pathway, clavulanic acid biosynthesis, and linoleic acid metabolism (Fig. 10D).

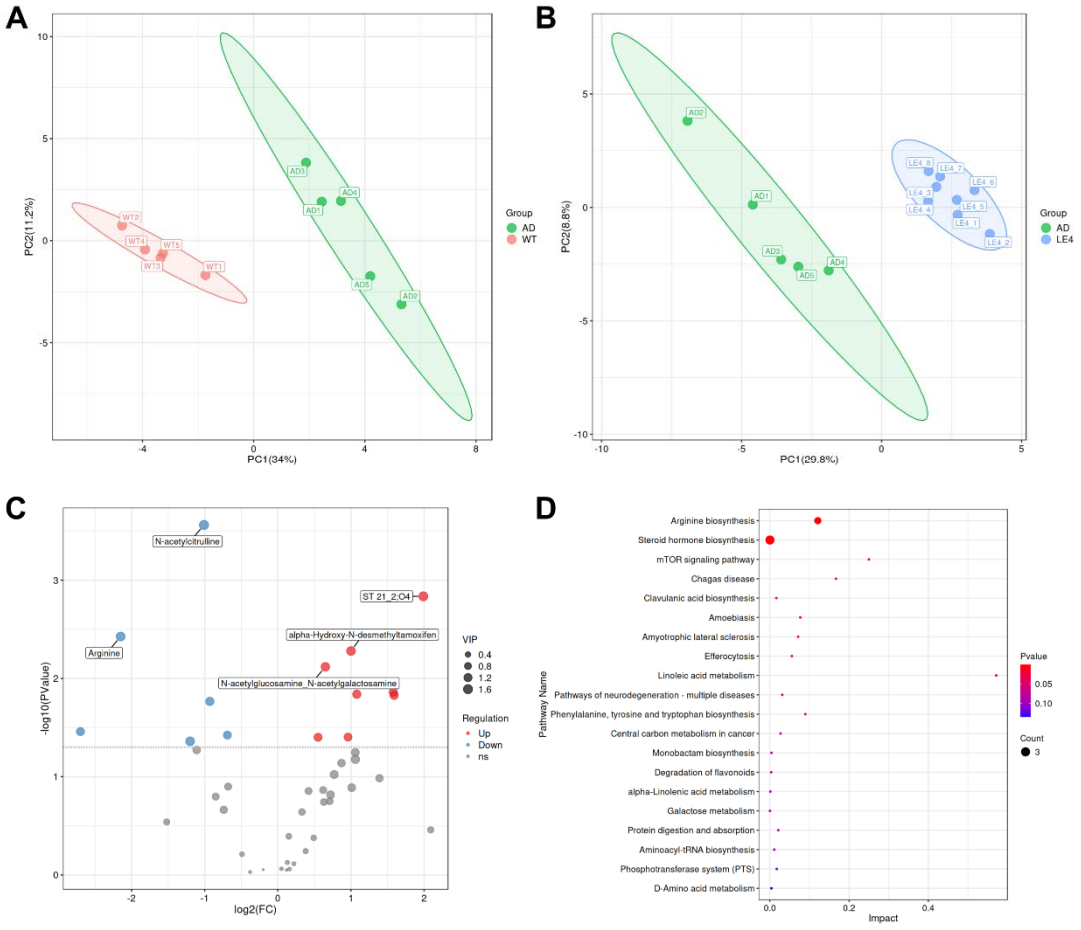

Fig. 10 Fecal Metabolomic Alterations and Pathway Analysis in APP/PS1 Mice Treated with *B. breve* LE4. (A, B) Partial least squares discriminant analysis (PLS-DA) score plots of fecal metabolomic profiles from WT, AD, and *B. breve* LE4-treated APP/PS1 mice. (C) Volcano plot displaying metabolite differences between AD and *B. breve*LE4 groups (VIP > 1.0, $P < 0.05$). (D) KEGG pathway enrichment analysis of differential metabolites between AD and LE4 groups (circle size: number of enriched metabolites; color scale: $\log_2$ fold change values).

Table 1. Differential fecal metabolites between the AD and ***B. breve*** LE4-treated groups.

ID	name	P value	FDR	VIP	Regulation
1	11-Dehydrocorticosterone	0.014829	0.079704	1.293876	Up
2	11a-Hydroxyprogesterone	0.039642	0.131125	1.183164	Up
3	13-Hydroxyabscisic acid	0.039502	0.131125	1.148766	Up
4	Arginine	0.003742	0.053638	1.491693	Down
5	Aromadendrin	0.014467	0.079704	1.281107	Up
6	FA 12_3;O (±)-JASMONICACID	0.01711	0.081747	1.309782	Down
7	Linoleic a	0.013773	0.079704	1.284153	Up
8	N-acetylcitrulline	0.000274	0.011782	1.669206	Down
9	N-acetylglucosamine_N-acetylgalactosamine	0.007607	0.065422	1.382639	Up
10	Protoanemonin	0.043572	0.133828	1.493024	Down
11	(24S,25)-Epoxycholesterol	0.001459	0.03136	1.577656	Up
12	Sanguinarine	0.037689	0.131125	1.156904	Down
13	Shikimic acid	0.034699	0.131125	1.187063	Down
14	alpha-Hydroxy-N-desmethyltamoxifen	0.005257	0.056515	1.457923	Up

FDR: false discovery rate.

VIP: Variable Important for the Projection.

$P < 0.05$ was considered significant.

3.10 B. breve LE4 ameliorates cognitive impairment in APP/PS1 mice by attenuating neuroinflammation through inhibition of the TLR4–NF-κB/NLRP3 signaling axis

B. breve LE4 intervention significantly reduced serum levels of LPS and IL-1β in APP/PS1 mice, implicating suppression of the TLR4/NF-κB signaling cascade. Western blot analysis revealed that hippocampal expression of TLR4 ($P < 0.01$), MYD88 ($P < 0.01$), IKKα ($P < 0.01$), and phosphorylated p65 (p-p65) ($P < 0.01$) was significantly downregulated following *B. breve* LE4 treatment, indicating inhibition of the canonical NF-κB pathway (Fig. 11A, C). In addition to NF-κB activation, APP/PS1 mice exhibited elevated hippocampal expression of NLRP3. To further assess the effect of *B. breve* LE4 on NLRP3-mediated neuroinflammation, we performed Western blotting of hippocampal tissue. *B. breve* LE4 treatment markedly reduced hippocampal levels of pro-caspase-1 p20 ($P < 0.01$), NLRP3 ($P < 0.01$), ASC ($P < 0.01$), and IL-1β ($P < 0.05$), consistent with ELISA data (Fig. 11B, D). These findings collectively suggest that *B. breve* LE4 exerts its neuroprotective effects by suppressing activation of the NLRP3 inflammasome and attenuating neuroinflammatory signaling via the TLR4–NF–κB/NLRP3 pathway.

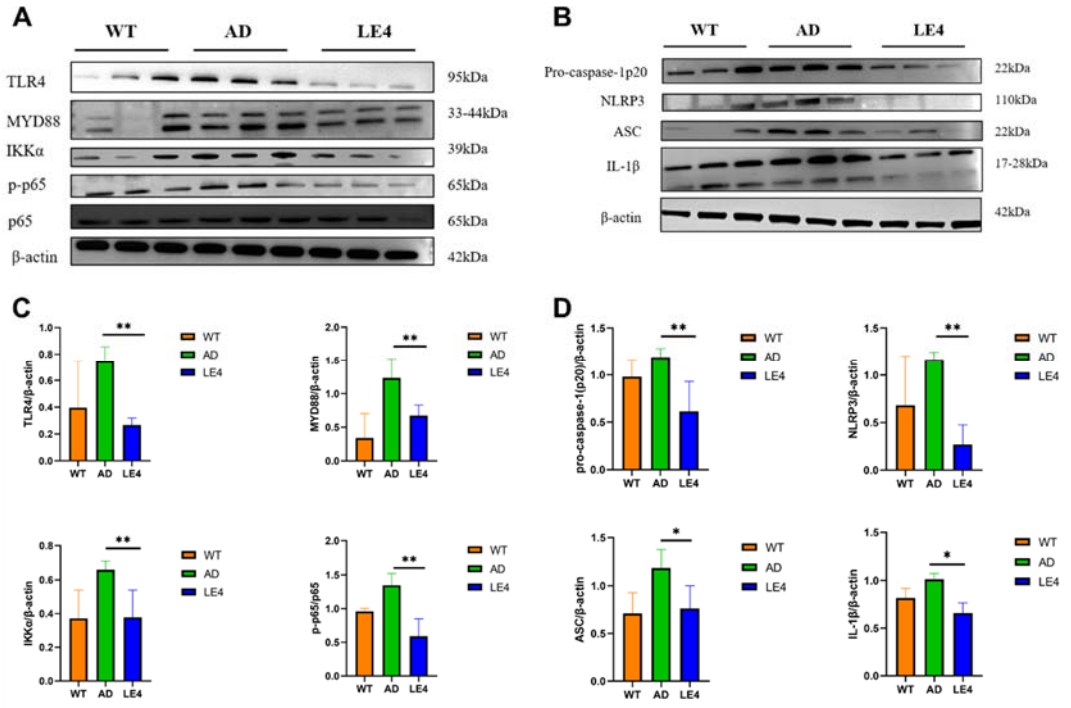

Figure 11. *B. breve* LE4 suppresses neuroinflammation by inhibiting the TLR4–NF–κB/NLRP3 signaling pathway in APP/PS1 mice. (A) Representative Western blot bands showing expression levels of TLR4, MYD88, IKKα, phosphorylated p65 (p-p65), and total p65 in the hippocampus of WT, AD, and *B. breve* LE4-treated mice. (B) Western blot bands for NLRP3 inflammasome-associated proteins, including NLRP3, ASC, pro-caspase-1 p20, and IL-1β in hippocampal tissue. (C) Quantification of the relative protein expression levels of the TLR4–NF–κB pathway components. (D) Quantification of NLRP3 inflammasome-associated protein expression. All protein levels were normalized to β-actin. Data are presented as mean ± SEM (n = 3). Statistical significance was determined by one-way ANOVA with Tukey's post hoc test. *$P < 0.05$, **$P < 0.01$ compared with AD group.

4. Disscution

With global population aging becoming a common issue worldwide, AD has emerged as an increasingly serious public health concern[1]. Currently, the treatment of AD remains a major challenge in the medical field. Although there is still no cure for this disease, the deepening understanding of its underlying

mechanisms has led to the development of several pharmacological treatments, such as memantine and donepezil[8]. However, these drugs can only temporarily alleviate symptoms or slow disease progression, and long-term use often brings significant economic burdens and potential side effects for patients[30]. Recent studies have shown that probiotics, particularly Bifidobacterium species, hold great promise in the early intervention and treatment of AD[31-33]. Nevertheless, the mechanisms by which they exert their effects remain unclear. Therefore, screening *Bifidobacterium* strains with anti-AD potential is of great scientific significance and may offer new avenues for the prevention and treatment of AD[34]. In our study, we screened 18 strains of *Bifidobacteria* and identified one strain, *Bifidobacterium breve* LE4, that effectively ameliorated AD-related symptoms. We further explored the potential mechanisms by which *B. breve* LE4 improves cognitive function in APP/PS1 transgenic mice.

One of the key features observed in both AD patients and animal models is gut microbiota dysbiosis[35]. This imbalance often leads to excessive production of LPS, contributing to intestinal inflammation and exacerbating systemic chronic inflammatory responses[36]. *Bifidobacteria*, a dominant probiotic genus in the gut, possesses anti-inflammatory properties[37]. However, its relative abundance declines with age[38]. Therefore, supplementation with *Bifidobacterium* may help suppress intestinal and systemic inflammation[37, 39]. Given the strain-specific properties of *Bifidobacterium*, we initially screened 18 strains isolated from the feces of healthy infants and evaluated their *in vitro* antioxidant activities. The five strains showing the best antioxidant performance were selected for subsequent *in vitro* LPS elimination experiments. LPS, a component produced by Gram-negative bacteria, serves as a marker of intestinal dysfunction. It increases the permeability of tight junctions in the intestinal epithelium and disrupts barrier integrity, allowing paracellular translocation of LPS into the intestinal lumen[40]. This triggers uncontrolled expression of pro-inflammatory cytokines and aggravates intestinal inflammation. Therefore, the ability of probiotic strains to inhibit LPS production during *in vitro* fermentation with mouse feces may indicate the potential to reduce gut inflammation[41]. Among the five strains with strong antioxidant capacity, *Bifidobacterium breve* LE4 showed the highest LPS-eliminating ability. However, since *in vitro* fecal fermentation models only partially simulate the gut environment and cannot fully reflect in vivo effects, it is necessary to conduct further in vivo experiments using *B. breve* LE4 in APP/PS1 transgenic mice.

Animal models are essential and irreplaceable tools for studying the fundamental mechanisms of AD pathology, as well as for drug development, prevention, and therapeutic interventions[42]. Among them, APP/PS1 transgenic mice are widely used because they effectively replicate core pathological features of human Alzheimer's disease, including behavioral deficits, cognitive impairment, and synaptic dysfunction. Behavioral testing is a critical approach to assessing cognitive improvement. In this study, we employed the Morris water maze[43], open field test[44], and nest-building test [45] to evaluate cognitive performance, anxiety-like behaviors, and activities of daily living, respectively. These tests provided a comprehensive overview of the therapeutic efficacy of *Bifidobacterium breve* LE4 in slowing disease progression. Although previous studies have reported the cognitive benefits of probiotic interventions in various AD mouse models,

the neuroprotective effects of probiotic administration remain elusive. The Morris water maze is considered the gold standard for assessing hippocampus-dependent spatial learning and memory in rodents[46]. In addition, the open field test and nest-building test are valuable tools for evaluating spontaneous activity and anxiety-related behavior in AD mice. After 12 weeks of *B. breve* LE4 administration, APP/PS1 mice exhibited significant improvements in cognitive function, reduced anxiety-like behaviors, and enhanced daily activity performance. These findings suggest that probiotic intake may alleviate behavioral impairments associated with AD. However, while *B. breve* LE4 improved multiple behavioral parameters; the underlying mechanisms by which it exerts these effects require further investigation.

Dysregulation of glucose and lipid metabolism is closely associated with AD pathology[47, 48], particularly through its impact on energy homeostasis and the neuroinflammatory microenvironment. Epidemiological studies have shown that abnormal body weight and impaired glycemic control in middle-aged and elderly individuals significantly increase the risk of AD progression[49]. Similar trends have been observed in AD mouse models, where metabolic disturbances exacerbate neuropathological features, while alleviating these disturbances can substantially improve disease outcomes[50]. For instance, curcumin has been reported to ameliorate AD pathology induced by high-fat and high-sugar diets by modulating hepatic lipid metabolism and reshaping the gut microbiota composition[51]. These findings highlight the importance of improving metabolic homeostasis as a therapeutic strategy in AD. In the present study, we observed that APP/PS1 mice exhibited significantly higher body weight compared to wild-type controls. Notably, *B. breve* LE4 administration markedly reduced body weight during weeks 3–10 of the intervention. This effect was consistent with a reduced liver index and histopathological improvement in hepatic tissues. Serum lipid profiles also showed significant reductions in TC and TG, indicating a modulatory effect of *B. breve* LE4 on lipid metabolism. Some researchers have proposed that AD may be considered a form of "type 3 diabetes" due to shared insulin signaling impairments[52]. Consistent with this theory, AD mice in our study displayed an increased trend in water intake and elevated fasting and postprandial blood glucose levels, albeit within normal ranges. *B. breve* LE4 supplementation helped restore both body weight and blood glucose levels, and also improved key markers of glucose metabolism, including GLP-1 and INS. Both GLP-1 and INS play crucial roles in regulating glucose homeostasis and have been implicated in AD mitigation by enhancing brain insulin signaling, reducing neuroinflammation[53, 54], and decreasing amyloid-beta deposition, ultimately leading to improvements in cognitive function.

Neuroinflammation plays a central role in the onset and progression of AD, as demonstrated by its close association with Aβ deposition[55], tau hyperphosphorylation, and microglial dysfunction. APP/PS1 transgenic mice, a widely used AD model, exhibit chronic systemic and neuroinflammatory responses. In this study, we assessed inflammatory markers in serum, hippocampus, and colon to evaluate the anti-inflammatory effects of *B. breve* LE4. Following 12 weeks of *B. breve* LE4 intervention, APP/PS1 mice showed significantly decreased levels of the pro-inflammatory cytokine IL-1β and increased levels of the anti-inflammatory cytokine IL-22 in serum, indicating a systemic shift toward an anti-inflammatory state.

Similarly, in the hippocampus, *B. breve* LE4 treatment markedly suppressed the expression of IL-1β and the NLRP3 inflammasome, while upregulating IL-22 levels, consistent with serum findings. Given that gut barrier integrity deteriorates with age in APP/PS1 mice, we further examined the gut inflammatory profile. LPS levels were significantly reduced in both serum and colonic tissues after *B. breve* LE4 supplementation. Immunofluorescence staining revealed restoration of tight junction integrity, supporting the notion that *B. breve* LE4 improves gut barrier function. Inflammatory mediators, such as LPS and cytokines, are capable of translocating across both the gut and blood-brain barriers, where they trigger neuroinflammatory cascades. Chronic neuroinflammation, primarily driven by NF-κB signaling, exacerbates oxidative stress, disrupts metabolic homeostasis, and accelerates neuronal degeneration[56, 57]. Western blot analysis confirmed that *B. breve* LE4 administration inhibited hippocampal NF-κB pathway activation, as well as the expression of NLRP3 and IL-1β, thereby attenuating central inflammation. This was further supported by immunohistochemical evidence showing that expression levels of Iba-1 and GFAP, markers for activated microglia and astrocytes, respectively, were significantly elevated in APP/PS1 mice but reduced following LE4 treatment. This suggests that *B. breve* LE4 ameliorates glial cell-mediated neuroinflammation.

The hallmark pathological features of AD include Aβ plaque deposition and hyperphosphorylated tau accumulation in the brain, both of which contribute critically to neurodegeneration[58, 59]. Importantly, our study found that the *B. breve* LE4 intervention significantly reduced Aβ accumulation and tau phosphorylation in the hippocampus of APP/PS1 mice. In addition, since synaptic plasticity is essential for learning and memory, we evaluated synaptic integrity. While compensatory increases in postsynaptic proteins were observed in the AD model[60, 61], *B. breve* LE4-treated mice exhibited improved dendritic spine morphology, potentially contributing to enhanced spatial memory precision. Increasing evidence indicates a strong association between gut microbiota dysbiosis and the pathogenesis of AD[35]. Gut microbes influence Aβ production and deposition in the brain and modulate tau phosphorylation through regulation of the host immune system and microbial metabolites[62], ultimately contributing to neuronal cytoskeletal disintegration and neurofibrillary tangle formation. The progression of AD has been shown to correlate directly with alterations in the gut microbiome. Moreover, intestinal microbes are now recognized as crucial modulators of the gut and central nervous systems, affecting the integrity of both the intestinal epithelial and blood-brain barriers[11].

In both AD patients and animal models, characteristic changes in gut microbiota composition have been observed. These include a reduced Firmicutes to Bacteroidetes (F/B) ratio and a threefold increase in the abundance of LPS-producing Proteobacteria[63]. Such dysbiosis exacerbates Aβ accumulation and tau hyperphosphorylation through host-microbiota metabolic interactions and promotes a cascade of neuroinflammatory responses. Disrupted gut microbiota can increase epithelial permeability, facilitating the translocation of microbial components that exacerbate neuroinflammation. In our study, AD model mice exhibited a significant decrease in alpha diversity and altered microbial composition, consistent with existing literature. The F/B ratio was increased in the AD group, whereas *B. breve* LE4 supplementation significantly

reduced this ratio and increased alpha diversity. A higher F/B ratio is generally associated with metabolic disturbances and systemic inflammation. Therefore, the *B. breve* LE4-mediated normalization of this ratio suggests a potential role in restoring microbial homeostasis. Interestingly, the relative abundance of *Lactobacillus* and *Bifidobacterium* genera increased in AD mice[64], possibly as a compensatory response to chronic pathological stress. This adaptive remodeling may reflect attempts by the microbiota to modulate inflammation, improve metabolic balance, and restore gut-brain axis homeostasis. However, elevated levels of specific *Lactobacillus* species have also been associated with enhanced microglial activation and pro-inflammatory cytokine release, exacerbating neurodegeneration[65]. *B. breve* LE4 intervention led to a favorable modulation of gut microbiota, characterized by increased relative abundance of *Allobaculum*, *Adlercreutzia*, and *Ruminococcus*. Previous studies have shown that *Allobaculum* is typically decreased in AD mice, and its abundance is inversely correlated with serum LPS levels. Restoration of *Allobaculum* may help reduce gut permeability and mitigate microglial activation. *Adlercreutzia* has been reported to negatively correlate with AD risk and may inhibit microglial IL-1β secretion. Metagenomic analysis suggests that *Ruminococcus* promotes the production of secondary bile acids, such as lithocholic acid, which activate the intestinal FXR receptor and inhibit Aβ deposition in the brain[66]. Furthermore, *B. breve* LE4 supplementation reduced the abundance of *Bacteroides*, a genus identified as an AD risk factor. *Bacteroides* can secrete neuraminidase, which cleaves E-cadherin, disrupts epithelial barrier integrity, and activates the NLRP3 inflammasome[67]. Collectively, our results demonstrate that *B. breve* LE4 intervention reshapes the gut microbiota toward a more favorable composition, potentially restoring intestinal barrier integrity, reducing systemic and neuroinflammation, and ultimately alleviating AD-related pathology.

The role of gut microbiota-derived metabolites in modulating AD pathology is increasingly recognized, with short-chain fatty acids (SCFAs) emerging as central mediators in microbiota–gut–brain axis communication[17, 68]. Dysbiosis observed in AD patients and transgenic mouse models, such as APP/PS1 mice, is consistently characterized by reduced abundance of SCFA-producing genera, including *Roseburia* and *Faecalibacterium* [69, 70]. This reduction is closely associated with compromised intestinal barrier integrity, heightened neuroinflammation, and cognitive impairment. In our study, *B. breve* LE4 intervention significantly increased SCFA levels, including acetate, propionate, and butyrate, which aligns well with previous findings. Similarly, supplementation with *Clostridium butyricum* elevated fecal butyrate concentrations by 2.8-fold, restored colonic tight junction protein claudin-3 expression to 1.8 times normal levels, and reduced hippocampal Aβ plaque burden by 35%[71]. The neuroprotective effects of butyrate appear to be mediated through multiple pathways. One mechanism involves histone deacetylase (HDAC) inhibition, which upregulates BDNF expression and supports synaptic plasticity. Another involves activation of the free fatty acid receptor 2 (FFAR2), enhancing microglial Aβ clearance efficiency[72]. Of note, propionate exhibits a dose-dependent effect. Low-dose sodium propionate (2 mM) significantly improved cognitive performance in APP/PS1 mice, as evidenced by a 30% reduction in escape latency in the Morris water maze. In contrast, high doses (>5 mM) induced microglial M1 polarization via the G protein-coupled

receptor 41 (GPR41), resulting in a 2.3-fold increase in IL-1β secretion[73]. This biphasic response has also been validated in the 3xTg-AD mouse model, emphasizing the importance of concurrent microbiota modulation to mitigate potential adverse effects of propionate. For instance, *Bifidobacterium animalis* subsp. *lactis* GCL2505 has been shown to elevate cecal propionate by 1.8-fold through fiber fermentation, while simultaneously increasing $Foxp3^+$ regulatory T cell proportions, thereby suppressing TLR4/NF-κB signaling and mitigating neuroinflammation[74]. In the present study, SCFA-associated restoration of gut barrier function was clearly demonstrated. Butyrate enhanced the acetylation of histone H3K9, promoting the expression of tight junction proteins ZO-1 and occludin[73]. In DSS-induced colitis models, this intervention reduced serum FITC-dextran permeability by 35%. Acetate, on the other hand, activated goblet cell MUC2 secretion via GPR43 receptor signaling, thereby reinforcing the mucosal barrier against pathogenic adhesion[75]. These findings corroborate our observations of improved gut barrier function following *B. breve* LE4 treatment and further underscore the pivotal role of SCFAs in the gut-brain axis.

In addition to SCFAs, emerging evidence highlights the critical role of gut microbiota-derived metabolites in modulating AD pathology[76, 77]. Non-targeted metabolomics has uncovered a complex interplay between gut microbiota and cerebral metabolic networks, revealing key disruptions in glucocorticoid metabolism, amino acid homeostasis, and lipid regulation in the progression of AD[78, 79]. Probiotics, by selectively altering these metabolic pathways, have been shown to ameliorate neuroinflammation and synaptic dysfunction, offering novel molecular targets for AD intervention[77]. With respect to glucocorticoid metabolism, alterations in the levels of 11-dehydrocorticosterone (11-DHC) and 11α-hydroxyprogesterone have been implicated in AD pathology. In APP/PS1 mice, brain levels of 11-DHC were reduced by 30%, a decline that directly triggered TLR4/NF-κB signaling activation in microglia, thereby exacerbating neuroinflammation[80]. Intervention with *Lactobacillus brevis* significantly increased the abundance of *Roseburia*, resulting in a restoration of serum 11-DHC levels to 75% of wild-type levels, while concurrently suppressing hippocampal IL-6 mRNA expression[81]. In addition, 11α-hydroxyprogesterone was shown to induce tau dephosphorylation via progesterone receptor activation in the 3xTg-AD mouse model[82]. Supplementation with *Bifidobacterium animalis* subsp. *lactis* Probio-M8 restored this metabolite to 80% of normal levels and markedly improved spatial memory performance, as evidenced by reduced escape latency in the Morris water maze[83]. These findings underscore the dynamic regulation of glucocorticoid metabolites as a key link between gut microbiota and neuroinflammatory modulation. Amino acid metabolism also plays a pivotal role in AD-related neuropathology. In the prefrontal cortex of AD model mice, arginine levels were reduced by 40%, while N-acetylcitrulline levels increased by 2.1-fold—an imbalance associated with abnormal arginase I activity[84]. Administration of the multi-strain probiotic VSL#3 increased the abundance of *Bifidobacterium longum*, restoring the arginine/ornithine ratio to 85% of baseline and promoting hippocampal PSD95 expression[85]. Moreover, levels of N-acetylglucosamine/galactosamine in the brain were reduced by 50% in AD models, which correlated with increased blood–brain barrier (BBB) permeability. Probiotic intervention improved these levels by 60%, potentially through AMPK/mTOR pathway-mediated

autophagy activation, and reduced tau phosphorylation by 30%[86]. These results highlight the central role of amino acid metabolism in maintaining synaptic integrity and BBB function. Lipid metabolic dysregulation is another hallmark of AD. Linoleic acid concentration in the hippocampus was reduced by 40% in AD mice. This metabolite has neuroprotective properties via cyclooxygenase-2 (COX-2) inhibition, which decreases prostaglandin E2 synthesis and enhances PPARγ expression[86, 87]. Administration of *Lactobacillus plantarum* KY1032 restored linoleic acid levels to 80% of wild-type values and significantly reduced hippocampal IL-1β mRNA expression[88]. Additionally, elevated levels of (24S,25)-epoxycholesterol have been observed in the plasma of 3xTg-AD mice; this metabolite activates liver X receptor (LXR), thereby suppressing Aβ deposition[85]. Collectively, these findings reveal that specific gut microbiota–derived metabolites can act as signaling intermediaries between the gut and brain, modulating key pathological processes in AD. The ability of probiotic interventions to reshape metabolic profiles adds a critical dimension to gut–brain axis research and provides a promising avenue for targeted therapeutic strategies.

To elucidate the relationships between gut microbiota, their metabolites (SCFAs and untargeted differential metabolites), and biochemical parameters, we performed Spearman correlation analyses (Fig. 11). Only parameters demonstrating robust correlations were included in the association analyses. Our findings revealed that bacterial taxa with restored relative abundance in the *B. breve* LE4 group exhibited positive correlations with beneficial biomarkers, whereas differential bacterial species between the AD and WT groups demonstrated positive associations with inflammatory cytokines and related parameters. Notably, *Bifidobacterium*, identified as a differentially abundant genus in the *B. breve* LE4 group, exhibited significant negative correlations with serum inflammatory cytokines and brain tissue pro-inflammatory mediators (IL-1β, IL-18, NLRP3), as well as amyloid-β peptides (Aβ1-40 and Aβ1-42). Conversely, this genus demonstrated positive correlations with glucose metabolism markers (insulin and GLP-1) and negative associations with lipid parameters (total cholesterol and triglycerides). These findings align with established literature demonstrating the anti-inflammatory properties of *Bifidobacterium*, while additionally supporting its role in normalizing glucose and lipid homeostasis. Furthermore, *Bifidobacterium* abundance showed strong positive correlations with short-chain fatty acids (SCFAs), particularly butyrate, and significant positive associations with upregulated metabolites, including 24(S),25-epoxycholesterol, alpha-hydroxy-N-desmethyltamoxifen, N-acetylglucosamine, and N-acetylgalactosamine, while also correlating with N-acetylcitrulline and arginine.

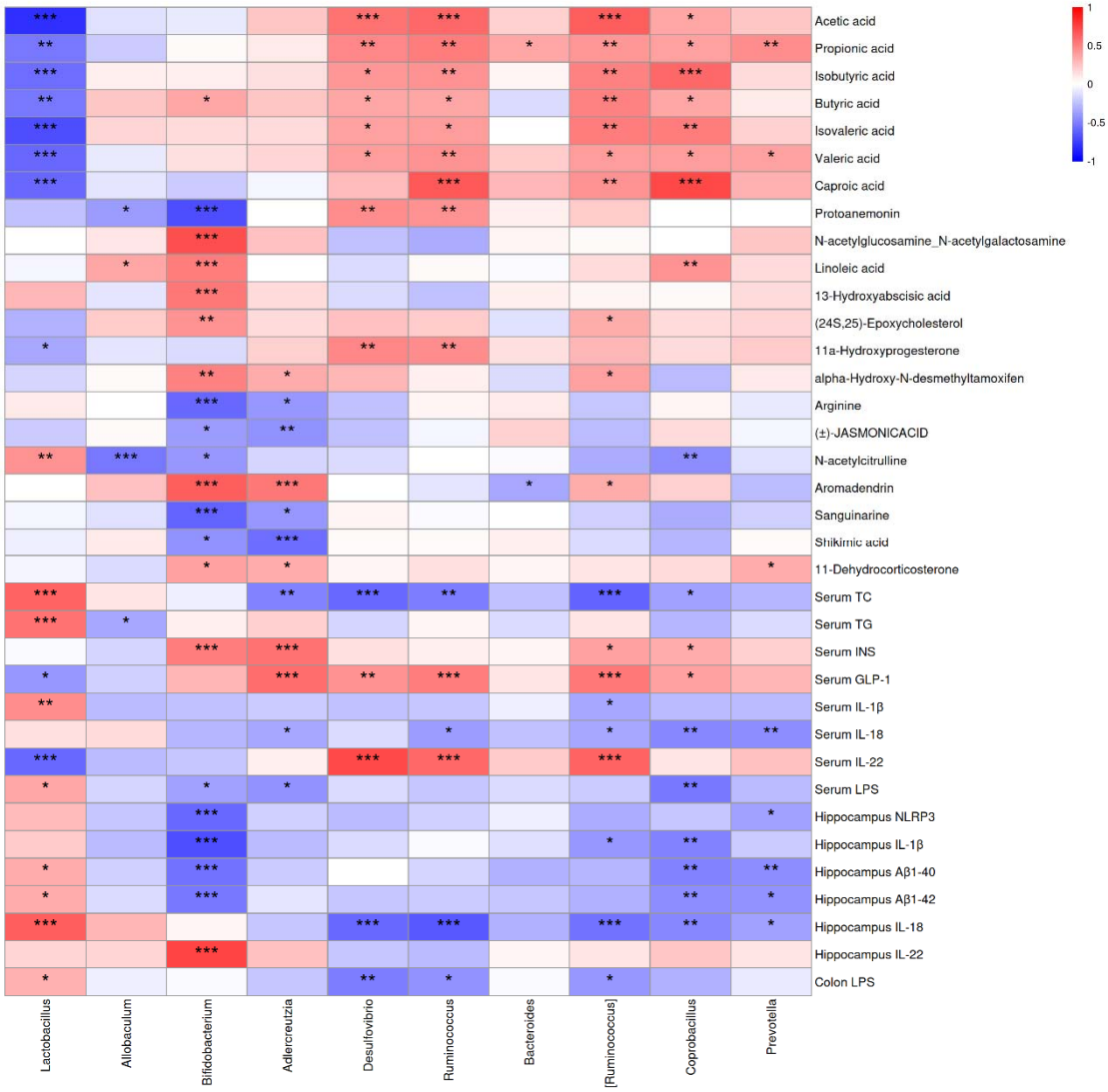

Fig. 12. Spearman correlation analysis.

Correlation analysis between differential gut microbiota and biochemical parameters, SCFAs, and key differential metabolites. The strength and direction of correlations are visualized with color intensity. *$P < 0.05$, **$P < 0.01$, and ***$P < 0.001$ indicate statistical significance.

Mechanistically, *Bifidobacterium* ameliorate AD-associated pathological markers through multiple metabolic pathways, including SCFA production, differential metabolite regulation, and microbiota composition optimization, thereby comprehensively modulating host lipid metabolism (Fig. 12). Additionally, despite their relatively low abundance, *Desulfovibrio*, *Ruminococcus*, *Bacteroides*, and *Coprobacillus* demonstrated positive correlations with SCFAs, potentially conferring neuroprotective effects against AD-associated cognitive decline through enhanced SCFAs production. Conversely, our analyses revealed that *Lactobacillus* abundance exhibited negative correlations with beneficial biomarkers and positive associations with inflammatory mediators, indicating the complex and bidirectional nature of *Lactobacillus* effects in neurodegenerative disease pathogenesis. The excessive proliferation of *Lactobacillus* may exacerbate AD pathogenesis through multiple deleterious pathways, including neuroinflammation activation, blood-brain barrier disruption, and compromised neuroprotective mechanisms. Consequently, aberrant *Lactobacillus* abundance may serve as a potential diagnostic biomarker for AD assessment.

4. Conclusion

This study systematically investigated the therapeutic potential of *Bifidobacterium breve* LE4 in APP/PS1 transgenic mice, a widely used model of AD. *B. breve* LE4 administration significantly improved cognitive performance and attenuated abnormalities in glucose and lipid metabolism. Additionally, *B. breve* LE4 effectively reduced systemic and neuroinflammatory responses, restored intestinal barrier function, modulated gut microbiota composition, and elevated SCFAs levels. Mechanistically, these effects were associated with the suppression of the TLR4–NF-κB/NLRP3 signaling pathway, reduced neuroinflammation, and enhanced synaptic plasticity. Untargeted metabolomics further revealed that *B. breve* LE4 regulates amino acid and lipid metabolic pathways, contributing to the mitigation of AD-like pathological features. Collectively, these findings suggest that *B. breve* LE4 exerts multi-targeted and multi-pathway effects, supporting its potential as a promising probiotic-based strategy for AD prevention and intervention.

Declaration of competing interests

The authors declare no potential conflicts of interest.

Reference

1. Philip, S., et al., *Alzheimer's disease.* The Lancet, 2021.
2. Joan, V.-F., et al., *Psychosis of Alzheimer Disease: Prevalence, Incidence, Persistence, Risk Factors, and Mortality.* The American Journal of Geriatric Psychiatry, 2013.
3. Alzheimer's Disease, I., et al., *World Alzheimer Report 2024: Global changes in attitudes to dementia*. 2024, Alzheimer's Disease International: London, England.
4. Anh, T., *Burden of caregiving to people living with dementia in low-and middle-income countries in Asia: a systematic review.* Alzheimer's & Dementia, 2023.
5. Denis, S.S. and G. Douglas, *Dynamics of neuroinflammation in Alzheimer's disease.* The Lancet Neurology, 2022.
6. Rabia, S., et al., *Pathogenesis of Alzheimer's Disease: Role of Amyloid-beta and Hyperphosphorylated Tau Protein.* Indian Journal of Pharmaceutical Sciences, 2018.
7. Camilla, F., et al., *PHARMACOLOGICAL TREATMENT OF ALZHEIMER'S DISEASE: AN INTEGRATIVE REVIEW ON THE EFFECTIVENESS OF CHOLINESTERASE AND MEMANTINE INHIBITORS.* International Journal of Health Science, 2023.
8. Robert, H., et al., *Donepezil and Memantine for Moderate-to-Severe Alzheimer's Disease.* The New England Journal of Medicine, 2012.
9. Naufal, K., et al., *Modulation of neuroinflammatory pathways by medicinal mushrooms, with particular relevance to Alzheimer's disease.* Trends in Food Science and Technology, 2020.
10. Weixin, L., et al., *Cost-effectiveness of physical activity interventions for prevention and management of cognitive decline and dementia—a systematic review.* Alzheimer's Research & Therapy, 2023.
11. Jian Sheng, L., et al., *Microbiota–gut–brain axis and its therapeutic applications in neurodegenerative diseases.* Signal Transduction and Targeted Therapy, 2024.
12. Seong Jin, J., et al., *Whole genome shotgun metagenomic sequencing to identify differential abundant microbiome features between dementia and mild cognitive impairment (MCI) in AD subjects.* Alzheimer's & Dementia, 2021.
13. Zhuoxin, L., et al., *Differences in Alpha Diversity of Gut Microbiota in Neurological Diseases.* Frontiers in Neuroscience, 2022.
14. Cátia Rodrigues de, A., et al., *Influence of gut microbiota dysbiosis on brain function: a systematic review.* Porto Biomedical Journal, 2020.

15. Paola, C.B.-M., et al., *Chronic-Antibiotics Induced Gut Microbiota Dysbiosis Rescues Memory Impairment and Reduces β-Amyloid Aggregation in a Preclinical Alzheimer's Disease Model.* International Journal of Molecular Sciences, 2022.
16. Kalyan, M., et al., *Role of Endogenous Lipopolysaccharides in Neurological Disorders.* Cells, 2022. **11**(24): p. 4038.
17. Xiaohang, Q., et al., *Mechanisms of Short-Chain Fatty Acids Derived from Gut Microbiota in Alzheimer's Disease.* Aging and Disease, 2022.
18. Moira, M., et al., *Short-Chain Fatty Acids and Lipopolysaccharide as Mediators Between Gut Dysbiosis and Amyloid Pathology in Alzheimer's Disease.* Advances in Alzheimer's disease, 2022.
19. Titikorn, C., et al., *P4–028 : PREBIOTICS, PROBIOTICS OR SYNBIOTICS THERAPY RESTORES COGNITIVE DECLINE IN OBESE RATS.* Alzheimer's & Dementia, 2017.
20. Dóra, Á., et al., *Exercise and probiotics attenuate the development of Alzheimer's disease in transgenic mice: Role of microbiome.* Experimental Gerontology, 2019.
21. Guangsu, Z., et al., *Environmental enrichment in combination with Bifidobacterium breve HNXY26M4 intervention amplifies neuroprotective benefits in a mouse model of Alzheimer's disease by modulating glutamine metabolism of the gut microbiome.* Food Science and Human Wellness, 2024.
22. Gu, Z., et al., *Bifidobacterium breve HH079 alleviates early-life antibiotic-exposed colon dysbiosis in mice by restoring the gut microbiota and gut barrier function.* Food & Function, 2025.
23. Yating, L., et al., *Bifidobacterium infantis and 2'-fucosyllactose supplementation in early life may have potential long-term benefits on gut microbiota, intestinal development, and immune function in mice.* Journal of Dairy Science, 2023.
24. Bo, Z., et al., *Bifidobacterium adolescentis CCFM8630 Exerts Anti-Obesity Effects by Modulating Gut Microbiota-Related Tryptophan Metabolism.* Deleted Journal, 2024.
25. Hongwon, K., et al., *Administration of Bifidobacterium bifidum BGN4 and Bifidobacterium longum BORI Improves Cognitive and Memory Function in the Mouse Model of Alzheimer's Disease.* Frontiers in Aging Neuroscience, 2021.
26. Yodai, K., et al., *P1-089: ADMINISTRATION OF BIFIDOBACTERIUM BREVE STRAIN A1 PREVENTS COGNITIVE IMPAIRMENT IN AN ALZHEIMER'S DISEASE MODEL MOUSE.* Alzheimer's & Dementia, 2018.
27. Yodai, K., et al., *BIFIDOBACTERIUM BREVE A1 SUPPLEMENTATION IMPROVED COGNITIVE DECLINE IN OLDER ADULTS WITH MILD COGNITIVE IMPAIRMENT: AN OPEN-LABEL, SINGLE-ARM STUDY.* The Journal of Prevention of Alzheimer's Disease, 2018.
28. Okubo, R., J. Xiao, and Y.J. Matsuoka, *Chapter 49 - Potential beneficial effects of Bifidobacterium breve A1 on cognitive impairment and psychiatric disorders*, in *The Neuroscience of Depression*, C.R. Martin, et al., Editors. 2021, Academic Press. p. 497-504.
29. Qian, X.H., et al., *Mechanisms of Short-Chain Fatty Acids Derived from Gut Microbiota in Alzheimer's Disease.* Aging Dis, 2022. **13**(4): p. 1252-1266.
30. The, L., *Lecanemab for Alzheimer's disease: tempering hype and hope.* The Lancet, 2022.
31. Linkai, Q., et al., *Microbiota-Gut-Brain Axis Dysregulation in Alzheimer's Disease: Multi-Pathway Effects and Therapeutic Potential.* Aging and Disease, 2023.
32. Mingxuan, Z., et al., *Probiotic Clostridium butyricum ameliorates cognitive impairment in obesity via the microbiota-gut-brain axis.* Brain, Behavior, and Immunity, 2024.
33. Lei, Q., et al., *Selenium Nanoparticles-Enriched Lactobacillus casei ATCC 393 Prevents Cognitive Dysfunction in Mice Through Modulating Microbiota-Gut-Brain Axis.* International Journal of Nanomedicine, 2022.
34. Xiaoyang, M., et al., *Alleviation of Cognitive Impairment-like Behaviors, Neuroinflammation, Colitis, and Gut Dysbiosis in 5xFAD Transgenic and Aged Mice by Lactobacillus mucosae and Bifidobacterium longum.* Nutrients, 2023.
35. Gudimetla, S. and K. Rahul, *Role of microbial dysbiosis in the pathogenesis of Alzheimer's disease.* Neuropharmacology, 2023.
36. Joshua, C., et al., *Microglia facilitate loss of perineuronal nets in the Alzheimer's disease brain.* EBioMedicine, 2020.
37. Samuel, J.G., et al., *Bifidobacterium mechanisms of immune modulation and tolerance.* Gut microbes, 2023.
38. Muriel, D., et al., *Insights into endogenous Bifidobacterium species in the human gut microbiota during adulthood.* Trends in Microbiology, 2022.

39. Yaqian, L., et al., *Bifidobacterium breve Protects the Intestinal Epithelium and Mitigates Inflammation in Colitis via Regulating the Gut Microbiota–Cholic Acid Pathway.* Journal of Agricultural and Food Chemistry, 2024.
40. Marcello, C., et al., *Interaction between Lipopolysaccharide and Gut Microbiota in Inflammatory Bowel Diseases.* International Journal of Molecular Sciences, 2021.
41. Ruchika, B., et al., *Lactic Acid Bacterial Supplementation Ameliorated the Lipopolysaccharide-Induced Gut Inflammation and Dysbiosis in Mice.* Frontiers in Microbiology, 2022.
42. Donna, M.W. and T.L. Bruce, *The importance of continuing development of novel animal models of Alzheimer's disease and Alzheimer's disease and related dementias.* Alzheimer s & Dementia, 2024.
43. Zachary, W., E.Y. Michael, and H. Stephanie, *Influence of aerobic exercise on cognitive function in the TgF344-AD model of Alzheimer's disease.* Physiology, 2023.
44. Claire, C., et al., *Bacteria isolated from the stools of Alzheimer's disease patients exacerbate cognitive impairment in a 3xTg AD mouse model.* Alzheimers & Dementia, 2021.
45. Annika, M., et al., *Lack of APP and APLP2 in GABAergic Forebrain Neurons Impairs Synaptic Plasticity and Cognition.* Cerebral Cortex, 2020.
46. Smitha, K., *Unraveling Early Signs of Navigational Impairment in APPswe/PS1dE9 Mice Using Morris Water Maze.* Frontiers in Neuroscience, 2020.
47. Kelly, T.D., B.J. Jordan, and D. Larry, *Insulin resistance in Alzheimer's disease.* Neurobiology of Disease, 2014.
48. Laura, B., et al., *Gut microbiota modulation in Alzheimer's disease: Focus on lipid metabolism.* Clinical Nutrition, 2022.
49. Butterfield, D.A. and H. Barry, *Oxidative stress, dysfunctional glucose metabolism and Alzheimer disease.* Nature Reviews Neuroscience, 2019.
50. Lucas, Z., et al., *The bile acid TUDCA improves glucose metabolism in streptozotocin-induced Alzheimer's disease mice model.* Molecular and Cellular Endocrinology, 2021.
51. Lamichhane, G., et al., *Curcumin Mitigates the High-Fat High-Sugar Diet-Induced Impairment of Spatial Memory, Hepatic Metabolism, and the Alteration of the Gut Microbiome in Alzheimer's Disease-Induced (3xTg-AD) Mice.* Nutrients, 2024. **16**(2): p. 240.
52. Alina Alerm, G., et al., *Glucose metabolism and AD: evidence for a potential diabetes type 3.* Alzheimer's Research & Therapy, 2022.
53. Kong, F., et al., *Glucagon-like peptide 1 (GLP-1) receptor agonists in experimental Alzheimer's disease models: a systematic review and meta-analysis of preclinical studies.* Frontiers in Pharmacology, 2023. **Volume 14 - 2023**.
54. Gejl, M., et al., *In Alzheimer's Disease, 6-Month Treatment with GLP-1 Analog Prevents Decline of Brain Glucose Metabolism: Randomized, Placebo-Controlled, Double-Blind Clinical Trial.* Frontiers in Aging Neuroscience, 2016. **Volume 8 - 2016**.
55. Kira, T. and S. Ben, *Inflammation biomarkers for future development of all-cause dementia, Alzheimer's disease, and vascular dementia.* Alzheimer's & Dementia, 2021.
56. Xue, G., et al., *Intestinal dysbiosis exacerbates susceptibility to the anti-NMDA receptor encephalitis-like phenotype by changing blood brain barrier permeability and immune homeostasis.* Brain, Behavior, and Immunity, 2024.
57. Mohammad Sobhan, K., et al., *The neuroprotective effects of targeting key factors of neuronal cell death in neurodegenerative diseases: The role of ER stress, oxidative stress, and neuroinflammation.* Frontiers in Cellular Neuroscience, 2023.
58. Jianguo, L., et al., *A pharmacological chaperone improves memory by reducing Aβ and tau neuropathology in a mouse model with plaques and tangles.* Molecular Neurodegeneration, 2020.
59. Athanasios, M. and K. Stefan, *Neurofibrillary tangles in Alzheimer's disease: elucidation of the molecular mechanism by immunohistochemistry and tau protein phospho-proteomics.* Neural Regeneration Research, 2016.
60. Yook, Y., et al., *Hyperfunction of post-synaptic density protein 95 promotes seizure response in early-stage aβ pathology.* EMBO reports, 2024. **25**(3): p. 1233-1255.
61. Geneviève, L., et al., *Postsynaptic density protein PSD-95 expression in Alzheimer's disease and okadaic acid induced neuritic retraction.* Neurobiology of Disease, 2008.
62. Shan, L., et al., *Gut Microbiota and Dysbiosis in Alzheimer's Disease: Implications for Pathogenesis and Treatment.* Molecular Neurobiology, 2020.

63. Heravi, F.S., K. Naseri, and H. Hu, *Gut Microbiota Composition in Patients with Neurodegenerative Disorders (Parkinson's and Alzheimer's) and Healthy Controls: A Systematic Review.* Nutrients, 2023. **15**(20): p. 4365.
64. Prajapati, S.K., et al., *Protection of Alzheimer's disease progression by a human-origin probiotics cocktail.* Scientific Reports, 2025. **15**(1): p. 1589.
65. Li, X., et al., *Lactobacillus rhamnosus GG ameliorates noise-induced cognitive deficits and systemic inflammation in rats by modulating the gut-brain axis.* Frontiers in Cellular and Infection Microbiology, 2023. **Volume 13 - 2023**.
66. Jia, W., et al., *Expert insights: The potential role of the gut microbiome-bile acid-brain axis in the development and progression of Alzheimer's disease and hepatic encephalopathy.* Medicinal Research Reviews, 2020. **40**(4): p. 1496-1507.
67. Devaux, C.A., S. Mezouar, and J.-L. Mege, *The E-Cadherin Cleavage Associated to Pathogenic Bacteria Infections Can Favor Bacterial Invasion and Transmigration, Dysregulation of the Immune Response and Cancer Induction in Humans.* Frontiers in Microbiology, 2019. **Volume 10 - 2019**.
68. Meirong, C., et al., *Ganmaidazao decoction alleviated cognitive impairment on Alzheimer's disease rats by regulating gut microbiota and their corresponding metabolites.* Arabian Journal of Chemistry, 2023.
69. Ling, Z., et al., *Structural and Functional Dysbiosis of Fecal Microbiota in Chinese Patients With Alzheimer's Disease.* Frontiers in Cell and Developmental Biology, 2021. **Volume 8 - 2020**.
70. Zajac, D.J., et al., *Exogenous Short Chain Fatty Acid Effects in APP/PS1 Mice.* Frontiers in Neuroscience, 2022. **Volume 16 - 2022**.
71. Sun, J., et al., *Effect of Clostridium butyricum against Microglia-Mediated Neuroinflammation in Alzheimer's Disease via Regulating Gut Microbiota and Metabolites Butyrate.* Molecular Nutrition & Food Research, 2020. **64**(2): p. 1900636.
72. Colombo, A.V., et al., *Microbiota-derived short chain fatty acids modulate microglia and promote Aβ plaque deposition.* eLife, 2021. **10**: p. e59826.
73. Qian, X.-h., et al., *Mechanisms of Short-Chain Fatty Acids Derived from Gut Microbiota in Alzheimer's Disease.* Aging and disease, 2022. **13**(4): p. 1252-1266.
74. Horiuchi, H., et al., *Bifidobacterium animalis subsp. lactis GCL2505 modulates host energy metabolism via the short-chain fatty acid receptor GPR43.* Scientific Reports, 2020. **10**(1): p. 4158.
75. Deleu, S., et al., *High Acetate Concentration Protects Intestinal Barrier and Exerts Anti-Inflammatory Effects in Organoid-Derived Epithelial Monolayer Cultures from Patients with Ulcerative Colitis.* International Journal of Molecular Sciences, 2023. **24**(1): p. 768.
76. Hang, Z., et al., *Xanthoceraside exerts anti-Alzheimer's disease effect by remodeling gut microbiota and modulating microbial-derived metabolites level in rats.* Phytomedicine, 2022.
77. Hyunjung, C. and M.J. Inhee, *Functional effects of gut microbiota-derived metabolites in Alzheimer's disease.* Current Opinion in Neurobiology, 2023.
78. Ihab, H., et al., *Untargeted metabolomics reveals sugar and homocysteine dysregulations in prodromal AD.* Alzheimer's & Dementia, 2020.
79. Emrin, H., et al., *Integrative metabolomics-genomics approach reveals key metabolic pathways and regulators of Alzheimer's disease.* Alzheimer's & Dementia, 2021.
80. Ding, S., et al., *Lactobacillus brevis Alleviates DSS-Induced Colitis by Reprograming Intestinal Microbiota and Influencing Serum Metabolome in Murine Model.* Frontiers in Physiology, 2019. **Volume 10 - 2019**.
81. Verma, M., et al., *11β-hydroxysteroid dehydrogenase-1 deficiency alters brain energy metabolism in acute systemic inflammation.* Brain, Behavior, and Immunity, 2018. **69**: p. 223-234.
82. Joho, D., et al., *Probiotic treatment with Bifidobacterium animalis subsp. lactis LKM512 + arginine improves cognitive flexibility in middle-aged mice.* Brain Communications, 2023. **5**(6).
83. Zhang, Z., et al., *Bifidobacterium animalis Probio-M8 improves sarcopenia physical performance by mitigating creatine restrictions imposed by microbial metabolites.* npj Biofilms and Microbiomes, 2024. **10**(1): p. 144.
84. Bergin, D.H., et al., *Altered plasma arginine metabolome precedes behavioural and brain arginine metabolomic profile changes in the APPswe/PS1ΔE9 mouse model of Alzheimer's disease.* Translational Psychiatry, 2018. **8**(1): p. 108.

85. Bonfili, L., et al., *Microbiota modulation counteracts Alzheimer's disease progression influencing neuronal proteolysis and gut hormones plasma levels.* Scientific Reports, 2017. **7**(1): p. 2426.
86. Naomi, R., et al., *Probiotics for Alzheimer's Disease: A Systematic Review.* Nutrients, 2022. **14**(1): p. 20.
87. Li, J., et al., *Gut Microbiome and Serum Metabolome Profiles of Capsaicin with Cognitive Benefits in APP/PS1 Mice.* Nutrients, 2023. **15**(1): p. 118.
88. Xiao-hang, Q., C. Si-yue, and T. Hui-dong, *Multi-strain probiotics ameliorate Alzheimer's-like cognitive impairment and pathological changes through the AKT/GSK-3β pathway in senescence-accelerated mouse prone 8 mice.* Brain, Behavior, and Immunity, 2024. **119**: p. 14-27.